ORGANIC DIODES IN DARK AND ILLUMINATED CONDITIONS

A THESIS

submitted by

KUNJ J PARIKH (EE10B125)

in partial fulfillment of the requirements
for the award of the degree of

BACHELOR OF TECHNOLOGY & MASTER OF TECHNOLOGY

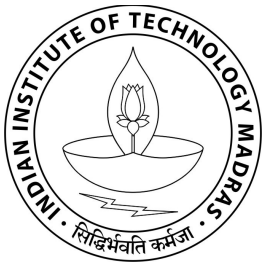

DEPARTMENT OF ELECTRICAL ENGINEERING
INDIAN INSTITUTE OF TECHNOLOGY MADRAS
MAY 2015

THESIS CERTIFICATE

This is to certify that the thesis titled **ORGANIC DIODES IN DARK AND ILLUMINATED CONDITIONS**, submitted by **Kunj J Parikh**, to the Indian Institute of Technology Madras, Chennai for the award of the degree of **Bachelor of Technology and Master of Technology**, is a bona fide record of the research work done by him under our supervision. The contents of this thesis, in full part or in parts, have not been submitted to any other Institute or University for the award of any degree or diploma.

Dr. Debdutta Ray
Research Guide
Assistant Professor
Department of Electrical Engineering
IIT Madras 600 036

Place : Chennai

Dr. Shreepad Karmalkar
Research Guide
Professor
Department of Electrical Engineering
IIT Madras 600 036

Place : Chennai

Date: 06/05/2015

ACKNOWLEDGEMENTS

This project would not have been possible without the guidance and assistance of several individuals who contributed towards the completion of this project.

I am ever grateful to the my project guides Dr. Debdutta Ray and Dr. Shreepad Karmalkar, whose guidance and encouragement were of immense value to me in completing this work.They have helped me in both academic and personal levels.

ABSTRACT

KEYWORDS : Organic diodes; solar cell; Disordered material; Recombination; Carrier transport; Space charge

Simulations are carried out for a un-doped organic material in illumination. Models and theoritical approaches which are proposed to explain transport in diodes made of disordered materials like organic, a-Si were used. Hopping model for charge transport which includes temperature, field and carrier concentration effect, and simplified case of trap recombination were considered. Effects of changing various parameters like temperature, Metal-semiconductor barrier, length of device, Intensity of illumination were observed on current voltage characteristics, carrier distribution and recombination withinin the device. Recombination behaviour was matched with the proposed behaviour. Intensity behaviour seen to match only for specific regime.

For device simulation Atlas module of TCad Silvaco software was used. And for plotting and fitting Origin was used. Although the device was made in 2D, all the results were used in 1D, along the line of absorption of light, from one contact to another.

TABLE OF CONTENTS

ACKNOWLEDGEMENTS **i**

ABSTRACT **ii**

LIST OF TABLES **iv**

LIST OF FIGURES **v**

1. **INTRODUCTION** **1**
2. **THEORY AND MODELLING** **2**
   - 2.1 Brief history of transport models 2
   - 2.2 Theoritical modelling of organic semiconductor 2
   - 2.3 Proposed models for disordered material 4
   - 2.4 Simulating software : Atlas 10
3. **RESULTS AND DISCUSSION** **14**
   - 3.1 Effect of Temperature on dark current 15
   - 3.2 Contact type and barriers 17
   - 3.3 Varying uniform photogeneration and recombination 19
   - 3.4 Recombination at different voltage bias 22
   - 3.5 Effect of device length 26
   - 3.6 Intensity effect on long device 29
4. **CONCLUSION** **35**

APPENDIX – ATLAS CODE **36**

REFERENCES **42**

LIST OF TABLES

2.1 : Values of parameters or their ranges considered for the simulations 14

3.1 : Contact workfunctions considered for various cases, and barriers thus formed 17

3.2 : Solar cell specific parameters obtained for constant photogeneration 21

3.3 : Solar cell specific parameters obtained for different lengths 28

LIST OF FIGURES

2.1: Typical device used for simulation. Light is incident from anode directed downwards. 13

3.1: Structure considered for dark current simulation. Anode-Organic-Cathode in order 15

3.2 : Dark current characteristics for various temperature, Semilog plot. 15

3.3 : Current vs Temperature for +5V 16

3.4 : Structure considered for contact effect simulation. Anode-Organic-Cathode 17

3.5 : Current Voltage characteristics for each case, plot is on semilog scale 18

3.6 : Current voltage characteristics in double logarithmic scale 18

3.7: Structure considered for constant photogeneration. Anode-Organic-Cathode 19

3.8 : Current voltage characteristics different photogeneration rates. Semilog plot 19

3.9 : Recombination rate(cm-3s-1) within the device, Semilog plot. 20

3.10 : Plot of current vs Intensity, double logarithmic scale 21

3.11 : Structure considered for bias' effect on recombination simulation. 22

3.12 : Band diagram for +2V(left) and -2V(right) 22

3.13 : Electron and hole concentration for different biases. Semilog plot 23

3.14 : Recombination through the device for different biases; linear plot. 24

3.15 : Structure considered for effect of device length simulation. 26

3.16 : Current voltage characteristics obtained for different device length; semilog scale 26

3.17 : Current voltage characteristics, power law fit for length effect study; double log scale 27

3.18 : Electron and hole concentration through device(s) overlaid; semilog plot 27

3.19 : Recombination Rate through the devices at different device length and bias 28

3.20 : Device considered for Intensity effect 29

3.21 : Current voltage (linear scale) observed for different intensities 30

3.22 : Current versus Intensity plot and linear fit for different Intensity range 30

3.23 : Band diagram within the device for different intensities; taken at 0V 31

3.24 : Electron and hole concentration within device for varying intensity; taken at 0V 32

3.25 : Electric field within the device for varying intensity; taken at -20V 32

3.26 : Current density within the device; taken at -20Vand -5V 33

CHAPTER 1
INDRODUCTION

Organic solar cells are gaining popularity because of being a renewable source of energy, lower fabrication temperatures than silicon counterparts, lower cost versus the cost of achieving pure crystalling Si, more variety of materials avaliable, properties like flexibility which can be important for certain applications. Ongoing research about understanding it's processes is increasing it's efficiency. Organic material is amorphous in nature and closely resembles a-Si (amorphous silicon) which is widely researched.

Things like energy distribution of carrier transport layers, mobility models for carriers, carrier recombination models, metal semiconductor contacts, process of absoption of light through intermediate excitonic entities, etc. are important in understanding any such device. Some of these proposed models will be dealt with here, the simulated characteristics can then be used to correlate with the data from fabricated devices to know their validity or to propose changes. Many of these models work well in specific regimes.

Solar cells based on conjugated polymers and fullerene compounds are promising candidates for solar energy converstion. One such material is MEH-PPV whose semiconducting parameters were taken at first, then tweaked to observe changes. For further simulations a bulk mix blend layer of MEHPPV-$PC_{60}BM$ was considered. A effective medium model[16](EMM) was considered for mix blend bulk hetrojunction structure, taking the HOMO of MEHPPV and LUMO of PCBM instead of 4 separate energy bands, although unlike as reported in the reference the mobilities of electrons and holes were kept same for our purposes, and other parameters like permittivity, N_t , etc. were kept either same as for MEHPPV case. Once these were fixed, some parameters were changed to observe their effects. Various metal contacts were used, starting with ITO as anode and Ca as cathode, but the workfunctions were changed to observe characteristics, and in some cases changed to suppress their effect and observe other effects, by making them injecting(to neglect injection limited current) or blocking(to decrease carrier concentration at electrode) as needed.

Software used for all simulations was Atlas, which has included Gaussian Disorder effects, recombination was modelled using external file.

CHAPTER 2
THEORY AND MODELLING

2.1 Brief history of Transport models[1]

Drude's model: Electrons accelerate under applied Electric Field and collide with lattice's heavy positive ions. This makes them scatter at random angle, and at a speed that on average was dependent on local temperature. Scattering sites were assumed to be lattice ions. It explained Ohm's Law and Joule heating effect.

Bloch waves: It included Quantum mechanical description of electron as a wave in a well-ordered periodic lattice. Scattering was considered to be because of defects, contaminations, and phonons. Free electrons mean whose mean-free path between subsequent collisions is longer than Bloch wavelength in that material.

Disorder: Anderson proposed that introducing disorder breaks crystal symmetry, wavefunctions are localized and energy states may be formed in forbidden energy gap. More about it is discussed in modelling and mobility discussion.

2.2 Theoritical modelling of Organic semiconductor[1]

A organic film is made up of polymer chains which are electrically broken by physical and chemical defects into further smaller conjugation units. Each of this subunit acts as a host of charge, and these subunits are spread throughout the space and energy dimension in polymer film.

These semiconductors have delocalized electrons in terms of pi bond electrons, which exist in many organic compounds due to carbon hybridization and it's bonding with other atoms. If we look at how molecules are formed from atoms, we see that as per molecular orbital theory there is energy splitting of various levels, for example π and π^* molecular orbital, the molecular orbitals of interest to us are the “lowest unoccupied molecular orbital” (LUMO) and “highest occupied molecular orbital”(HOMO). As more and more moleculars come together, due to local variartions and it's interaction with each other, they get distributed in energy. In silicon, due to strong inter atomic bonds it forms a crystal and the distribution forms a well defined band structure whose edge we define for semiconductor properties.

While in organic material,small molecular subunits themselves are formed of covalent bonds which are strong enough, but these subunits are held together by weak Van Der Walls' forces. Due to their weak nature, smallest of the physical or chemical effect can cause distortion in the energy of the bond that holds two subunits together. Also, these structures are affected by the polarization caused by charge in the neighbouring molecules, this polarization is nonuniform and causes distributed energy levels. Hence, as we go through the molecular film we observe that not all such weak bonds are of equal strength, and thus the intermolecular distance between these units is not constant. Also low strength bonds caused low wavefunction overlap. It is observed in the absorption of light by organic film that it is closely resembled by absorption by liquid phase than a solid crystal, in being distributed across various wavelength, this shows disorder in structure.

Even the bands formed in molecular crystals, unlike the crystalline silicon, are narrow due to low wavefunction overlap. It behaves as in the case of tight binding model, if a picture of electrons and ions is imagined, the electron when captured by an ion primarily orbits around the ion unaffected by other ions. If we talk in terms of Bloch funtion say, $\psi_k(x)=\frac{1}{N^{1/2}}\Sigma_{j=1}^{N} e^{ikX_j}\phi_v(x-X_j)$ [2] where X_j is the center of the j^{th} atom, the function Φ decays rapidly away from X_j, such that it becomes negligible even at X_{j+1}; this is because of low wavefunction overlap. This is the assumption of Tight Binding model.

The organic thin films used for these solar cells are amorphous and dont form bands too, their energy levels are not sharply defined but proposed to follow gaussian distribution around a particular energy, the width of gaussian is normally between 50-150meV. There are models which propose exponential distribution of tail states of the transport levels, but we will not consider them here. It is proposed also that these tail states may overlap with the impurity created localized states within the bandgap. A concept of mobility edge is then needed which forms a boundary between them, as the mobility will be less in the localized states than the delocalized ones. Then a The parabolic density of states related to band model for crystalline semiconductors was derived from Schrodinger equation assuming periodic lattice which isn't the case here so it can't be used.

When the charge is placed among molecules, as mentioned earlier they get polarized each forming a small dipole, these dipoles get arranged to screen the charge. It takes some time for the neighbouring molecules to reach this state and the polarization cloud to form. This time is called electronic polarization time τ_{el} . There is anoter time called residence time τ_{res} which corresponds to the average time charge will reside on the molecule. Also the mobility of carriers is proportional to

bandwidth of HOMO and LUMO thus formed, $\mu_h \sim \Delta E_{HOMO}$. And thus the mobility of carriers is less in organic semiconductors too. For polaron to form, that is polarization effect to take effect and become dominant principle, $\tau_{el} < \tau_{res}$, that is charge should stay there while polaron is formed. This time scales are related to bandwidth of energy following Heisenberg's principle. $\tau \leq \frac{\hbar}{\Delta E} \sim \mu^{-1}$

As seen, ΔE for organic molecules is less, and thus τ_{res} two orders more. And the τ_{el} now becomes less than τ_{res}.[3] Thus due to polarization effect band transport model can't be used.

Single crystal Si solar cells have usually low absorption coefficients and are thick filmed, so the limiting factor is the diffusion of carriers through the low field region, and not the transport through the high field junction. While in a-Si:H or organic solar cells, having large absorption coefficients, thin film cells can be made which have high field region throughout the cell. Thus diffusion plays a minor role in comparision to field led drift transport.

2.3 Proposed models for disordered material

Basic equations used to solve the state of the device with respect to carriers are as follows. The equations are mentioned for holes, they are similar for electrons.

Current equation for holes : $J_p = e\mu_p (Ep - V_T \, dp/dx)$

Continuity equation for holes : $\frac{dp}{dt} = \frac{-1}{e}\frac{dJ_p}{dx} + G - R$

Poisson equation : $\varepsilon \frac{dE}{dX} = Q_s + e(p - n)$

Below is the density of states assumed for crystalline semiconductors, for which band transport model is used. It is derived using Schoddinger equation in periodic lattice environment.

- Parabolic Density of states:

$$N(E)dE = \frac{\sqrt{2}}{\pi^2}\left(\frac{m}{\hbar^2}\right)^{3/2} E^{1/2} dE$$

Here N is the number of states present at the energy E per unit volume, m is the effective mass of the carrier. As can be seen N is proportional to $E^{1/2}$, hence the name.

- Gaussian Desity of states:

As mentioned earlier, we used Gaussian density of states to model disordered semiconductors it is found to correspond with the absorption spectra., and to the fact that polarization energy is dependent upon location of molecules, which vary by small amounts within the film.

$$N_C(E) = \frac{N_{t,n}}{\sqrt{2\Pi\sigma_n^2}} \exp\left(\frac{-E_n^2}{2\sigma_n^2}\right)$$

Here N_C is density of states which correspond to electron transport layer or the LUMO. E_n is measured with respect to the center of the gaussian distribution. N_t is the total number of "hopping sites" avaliable. σ is the standard deviation of the gaussian spread.

$$N_{t,n} = \frac{1}{A_n^3}$$

Total density of sites is related to average distance between sites by the above formula.

$$\alpha_n = \frac{10}{A_n}$$

The average distance is related to inverse of electron localization length in this manner. This will appear in mobility model later. As reported by Pasveer et al. this factor of 10 is true for relavant polymers, and that changing α changed prefactor of mobility.

For our simulations we will specify values of $N_{T,n}$, $N_{T,p}$, σ_n , σ_p ; respective A and α will be calculated based on it.

- Caughey Thomas model for Temperature dependence:[4]

$$\mu_{n0} = \mu_{min}\left(\frac{T_L}{300\text{K}}\right)^{\alpha_n} + \frac{\mu_{max}*\left(\frac{T_L}{300\text{K}}\right)^{\beta_n} - \mu_{min}*\left(\frac{T_L}{300\text{K}}\right)^{\alpha_n}}{1+\left(\frac{T_L}{300\text{K}}\right)^{\gamma_n}\left(\frac{N}{N_{crit}}\right)^{\delta_n}}$$

The parameters used in this equation can be user defined but for this case, default values, which are derived for Si were used. This model's temperature dependence was then used to simulate the device across the range of temperatures. As explained in their paper, the values of parameters are found by fitting obtained characteristics.

- Mobility:

The type of mobility model considered here is Hopping mobility. There are another, one another

that appears frequently is mobility considering polaronic effects, they won't be discussed or used here.

The density of states of these materials is such that the tails of density of states extend within the bandgap, and localized states due to other defects can be found within the bandgap. Sometimes the extended states overlap with the localized states and then the concept of mobility edge (or mobility gap) is used to differentiate between the two overlapping types of states. The transport in extended states is better than the localized states.

In crystalline material shallow or deep traps may be present, which are considered localized, that is the carrier caught in it will not contribute to current. While in disordered material we need to consider the contribution of current due to hopping of this carriers from one trap state to another. For we will see that even in HOMO, LUMO, which are considered to be having gaussion density of states, we see this type of transport; that there is not a continuous band but the carriers hop from one site to another. This sites are spread in space dimention and energy dimension both.

Master equation describes this process of hopping as follows :[1]

$$\frac{\partial}{\partial t} f_i(t) = -\Sigma_{j \neq i} W_{ji} f_j(t)[1 - f_i(t)] + \Sigma_{j \neq i} W_{ij} f_i(t)[1 - f_j(t)] - \lambda_i f_i(t)$$

Where $f_i(t)$ is the probability that the site i is occupied by carrier or excitation.

W_{ij} is the transition rate from site i to site j

λ_i is the decay rate of excitation at site i , or recombination.

Along with this is used Miller Abhraham's equation for transition rate for hopping. It is based on phonon assisted tunneling mechanism. For this model no polaronic effects are considered. Polaron model gives rise to a different W_{ij} .

This equation will have a $-eER_{ijx}$ term with the energy difference term if electric field is present.

$$W_{ij} = \nu_0 \exp(-2\gamma |R_{ij}|) \begin{cases} \exp\left(\frac{-(\varepsilon_j - \varepsilon_i)}{kT}\right) & \forall \varepsilon_j > \varepsilon_i \\ 1 & else \end{cases}$$

Here ν_0 is the phonon jump frequency,

γ is the inverse localization radius (Result of overlap of wavefunction. This is related to our N_t in simulations),

ε are the energy of the respective sites i and j,

R_{ij} is the distance between two sites.

In the work by H. Bassler[5], he performed Monte Carlo simulations for gaussian disorder model and the mobility obtained showed non-Arrhenius temperature dependence specifically :

$$\mu \propto \exp(-c\,\hat{\sigma}^2),\quad c \approx 0.44,\quad \hat{\sigma} = \frac{\sigma}{kT}$$

where σ is the width of the gaussian.

While in limited field range Poole Frenkel behaviour with respect to field was found :

$\mu \propto \exp[\gamma\sqrt{E}]$ but for wider field range carrier concentration dependence was needed to explain the characteristics.

In the work by W. F. Pasveer et al[6] . they have iteratively solved these equations for a cubic lattice and following results were presented which included concentration dependence, combining with it the field and temperature relations from the other two authors.

Pasveer model[6] : (as used in Atlas)[7]

Mobility is presented in terms of three terms each dependent on a particular parameter.

$$\mu(T,n,E) = \mu_{300}\, g_0(T)\, g_1(n,T)\, g_2(E,T)$$ where,

$$g_{0,n}(T) = \exp\left[\frac{T_{C_2,n}\,\sigma_n^2}{k^2}\left(\frac{1}{300^2} - \frac{1}{T^2}\right)\right]$$

$$g_{1,n}(n,T) = \exp\left[\frac{1}{2}\left(\frac{\sigma_n}{k_B T}\right)\left(\frac{\sigma_n}{k_B T} - 1\right)\left(2\frac{n}{N_t}\right)^{\delta_n}\right]$$

where $$\delta_n = 2\left(\frac{k_B T}{\sigma_n}\right)^2 \left[\ln\left\{\left(\frac{\sigma_n}{k_B T}\right)\left(\frac{\sigma_n}{k_B T} - 1\right)\right\} - \ln(ln4)\right]$$

$g_{1,n}(n,T)$ is valid for $\frac{n}{N_{T,n}} \le n_{cutoff}$, else calculated at cutoff.

$$g_{2,n}(E,T) = \exp\left[0.4 * \left\{\left(\frac{\sigma_n}{k_B T}\right)^{3/2} - 2.2\right\} * \sqrt{1 + 0.8\left(\frac{q A_n E}{\sigma_n}\right)^2} - 1\right]$$

$g_{2,n}(E,T)$ is valid for $\frac{q A_n E}{\sigma_n} \le E_{cutoff}$ else calculated at cutoff.

For using this model in Atlas we specify the values of cutoff field and concentration for each carrier (taken same). T_c was taken as 0.42. Values of σ , A_n , N_T were taken from the values used while describing Gaussian DOS.

The earlier mentioned Poole Frenkel Mobility (which includes only the field effect) was used for one of the simulations the equations as used by Atlas are as follows:

$$\mu_n(E) = \mu_{n0} \exp\left[\frac{-\Delta_{En}}{k T_{neff}} + \left(\frac{\beta_{Ap}}{k T_{neff}} - \gamma_n\right)\sqrt{|E|}\right] \quad \text{where} \quad T_{neff} = \frac{T_{on} T_L}{T_{on} - T_L}$$

For this case β and Δ were specified, others taken as default values.

- Recombination models:

<u>Crandall recombination</u>:

A simple recombination model has been proposed by Crandall et al.[9] based on SRH recombination:

$$R = \frac{np}{n\tau_p + p\tau_n}$$

Trapping time for holes τ_p is defined as : $\tau_p^{-1} = N_r \langle v S_p \rangle$

where N_r is the density of recombination centers,

v is the thermal velocity of the carrier,

S_p is the capture crossection for the holes.

Lifetime of carrier τ_p^R is defined as : $\tau_p^R = \frac{p}{R}$

which gives $\tau_p^R = \tau_p\left[1 + \frac{\tau_n}{\tau_p}\frac{p}{n}\right]$

One can see that recombination lifetime is always more than the trapping time. It goes with the theory that both carriers need to reach the trap for the recombination to complete.

One of the carrier gets caught in the trap, recombination is complete when the other carrier

enters the trap. Hence say hole mobility is lower than electron mobility, drift length of holes is less than of electrons. That is electrons will travel a longer distance in field before they recombine. And it is this carrier, which has longer drift length which decides the behaviour of solar cell.

At anode due to work function and affinity differences, electron concentration is very less, while at cathode hole concentration is less. And it can be seen from the Recombination equation that

$if\ n \gg p\ \ than\ R = \frac{p}{\tau_p}$ and at the other electrode $R = \frac{n}{\tau_n}$. Therefore we can't make constant lifetime approximation over device, as recombination goes from hole to electron dominated.

Langevin recombination[10]

For low mobility disordered semiconductor, as the carriers are moving slow, there are chances of electron combining with neighbouring hole. While SRH recombination occures across the band catalyzed by the presence of trap level in the forbidden gap, here nearby carriers are attracted to each other by Coulombic attraction.

Say an electron is nearby a hole. Assume hole to be static, and electron moving with the relative speed. The current density of electron due to the drift caused by coulombic attraction by hole is given by : $J_e = q\, n \mu_n \left(\frac{q}{4\pi\varepsilon r^2}\right)$

Calculating the incoming flux of electrons over entire sphere around hole:

$$I_e = \frac{q^2 \mu_n n}{\varepsilon}$$

This gives the number of electrons trying to combine to the hole, we have p such holes and both are moving so take average of both mobilities.

$$I_e = \frac{q}{\varepsilon}\left(\frac{\mu_n + \mu_p}{2}\right) np$$

Thus we get this equations for Langevin recombination:

$$R(n, p) = r_L(x, y, t)(np - n_i^2)$$

$$r_L(x, y, t) = A_{Langevin} \frac{q[\mu_n(E) + \mu_p(E)]}{\varepsilon_r \varepsilon_0}$$

$A_{langevin}$ is by default 1 in the Atlas simulator. This model for recombination was giving convergence error for me when used along with Gaussian DOS and Hopping mobility.

- Other equations used :

For all simulations Im(η) was specified and it was used to calculate absorption coefficient α the relations used for it was : $\frac{\alpha}{2}=\frac{\omega}{c}\eta_{Imag}$ or $\eta_{imag}=\frac{\lambda\alpha}{4\pi}$ where wavelength of light was chosen depending upon energy gap by $\lambda=\frac{\hbar c}{q E_g(eV)}$

Fill Factor of solar cell $FF=\frac{P_{maximum}}{I_{SC} V_{OC}}$

Space charge limited current[11] : $I=\frac{9\epsilon\mu V^2}{8L^3}$

2.4 : Simulating software : Atlas[7]

The device simulation piece of code is written in a generally fixed format. It will be mentioned here briefly in order. One example code used for a set of results is presented in appendix with comments.

- Structure specification:

Variable or constant definations using set or assign statements. For example x is defined as 5 here, and is used multiple times inside. It can be changed from here. Constants like Boltzman constant, etc.

Mesh : It consists of horizontal and vertical lines, which together form a grid which will make the physical device. Dimensions, spacing for accuracy vs speed are defined as per need. The coordinates in 2D are as if we are working in 4th quadrent.

Region : This part of the code assigns different portions of the mesh to different material (Si , organic, insulator, etc.). The region is specified using dimensions, and is labelled for further use.

Electrode : Electrode dimensions, names, numbers are assigned by this statement. It should be a part of mesh too.

Doping : This part defines the doping (uniform, gaussian or etc.) for different areas defined as

any semiconductor in region statement. Dimensions, junction depth, N_D, etc. are used. For undoped semiconductor this statement may be absent.

- Material and model specification:

Material : For each of the region specified as semiconductor earlier, this statement is used to define band gap, affinity, permittivity, N_c, N_v, [sigma], refractive index, absorption coefficient, etc.

Mobility : For organic semiconductor, various models can be used to simulate the device, eg. Poole frenkel type mobility, Pasveer model for mobility etc. The parameters for each respective needed model are specified here. Also μ_n and μ_p can be defined here.

Models : This statement specifies other models we want to consider like Langevien recombination, singlet dissociation model etc.

Beam : To simulate an incident beam, this statement is used. Coordinates of beam origin, beam width, wavelength, direction of propogation.

Contact : For each of the region defined as electrode earlier, workfunctions and other specifics related to electrodes can be specified here.

Probe : This statement can be used to probe various parameters at any point in the device. Specify point by coordinates, parameter probed by name.(eg. Electric Field)

Method : Here the numerical method we want to use to solve can be specified. For example, Newton, Gummel, etc.

- Solving and storing :

This part consists of 4 main statements which will be interspersed and out of order as and when required in the code.

Load: Using this statement we can load the previous saved solutions to be used as initial guesses for next solve statements.

Log: This statement can be used to specify the name of the file where we want to store results from upcoming solve statements for the entire bias sweep. Probed values are stored in log files too. Results stored are electrode currents, voltages, Illumination intensity etc.

Save: This statement can be used to specify the name of the file where we want to store the state

of the device as it is after the previous solve statement for one bias. It stores many more parameters like band edges, carrier concentration, carrier mobility etc.

Solve: This statement is used to specify the voltage, current, temperature, Intensity(of illumination), etc. sweeps.

- Plotting and extracting:

Extract: This can be used to analyze curves, for example I_{sc} from I versus V curve. Perform some mathematical operations to obtained values etc.

Tonyplot: This is to plot any log and save files to plot various parameters against each other and/or within the device.

Below is shown the typical organic diode used for our simulations. The electrodes were considered to be transparent metals, whose workfunction was changed based on need. Cathode was always kept at 0V bias and anode bias was sweeped. The mesh density in organic material was decreased or increased based on need for accuracy vs speed. The general properties of the organic material used will be provided in the table, and properties changed per case will be mentioned in the results section alongwith.

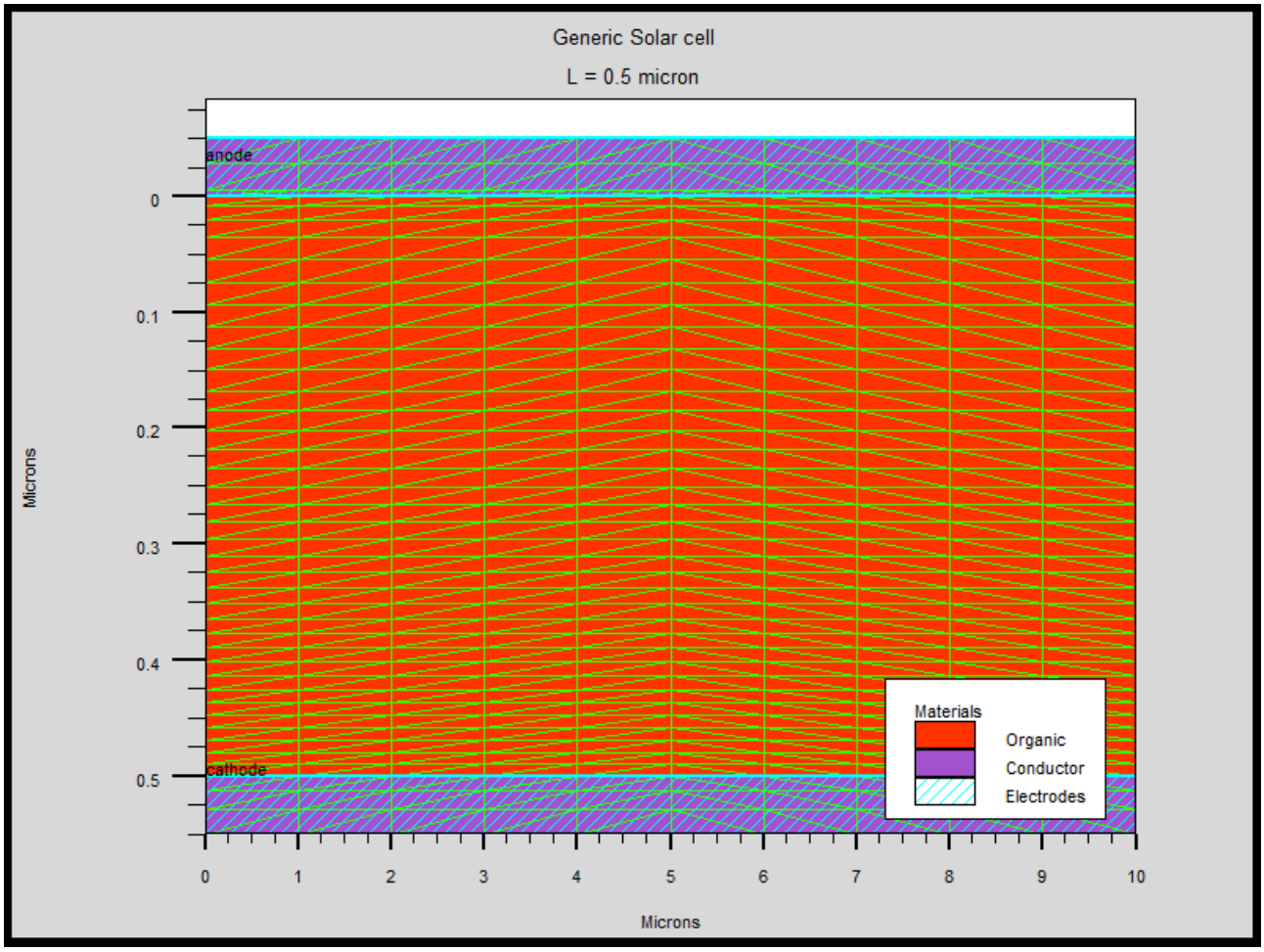

Figure 2.1: Typical device used for simulation. Light is incident from anode directed downwards.

Table 2.1 : Values of parameters or their ranges considered for the simulations.[7]

Symbol	Parameter	Value (Range)	Unit
$L_{organic}$	Length of organic material considered.	0.05-2	μm
$L_{contacts}$	Length of contacts	0.05	μm
$E_{g,300K}$	Band Gap at 300K	1.1,2,2.1	eV
ε_r	Relative permittivity	3	-
Nc, Nv	Effective Density of states (Parabolic)	$2.50x10^{19}$	cm^{-3}
χ	Electron Affinity of organic material	2.8-4.2	eV
Im(η)	Imaginary part of refractive index	$1.43x10^{-03}$-1.43	-
N_{tc}, N_{Tv}	Total DOS (Gaussian)	$8.51x10^{20}$	cm^{-3}
σ_c, σ_v	Standard Deviation of Gaussian DOS	0.05,0.08,0.155	eV
μ_{n0}, μ_{p0}	Low field mobility	10^{-4}	$cm^2V^{-1}s^{-1}$
λ	Wavelength of incident beam	0.5-0.9	μm
$W_{f,a}$	Workfunction of anode	4.2-5.3	eV
$W_{f,c}$	Workfunction of cathode	2.9-4.2	eV
I_b	Intensity of beam	0.01-1000	Wcm^{-2}
V_{anode}	Voltage at anode	(-20)-20	V
T	Temperature	100-350	K
α	Absorptin coefficient	f(Im(η))	m^{-1}
τ_R	Lifetime used in relation to Crandall recombination	10^{-6}	sec
E_{cutoff} (Pasveer)	Normalized Field limit	10	-
N_{cutoff} (Pasveer)	Normalized conc. limit	1	-

*For these simulations values of all parameters for electrons and holes are kept equal.

CHAPTER 3
RESULTS AND DISCUSSIONS

3.1 : Effect of Temperature on Dark current characteristics

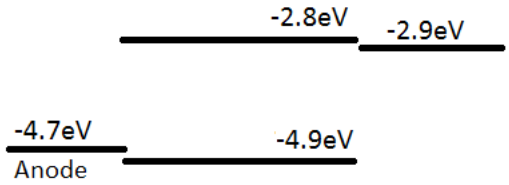

Figure 3.1 : Structure considered for dark current simulation. Anode-Organic-Cathode in order

For this part, Parabolic DOS which is used in Si was considered. N_c and N_v were considered equal, values as shown in the table.

Caughey-Thomas's model[4] for low-field mobility was used, which has Temperature dependence. This low-field mobility is used further in Poole-Frenkel mobility model[7] which has temperature dependence too.

Mobility was taken of Poole Frenkel nature, Δ_{an} , Δ_{ap} were taken equal to 0.48eV; β_{an}, β_{ap} were taken equal to $3.7\text{x}10^{-4}\text{eV}(\text{cmV}^{-1})^{1/2}$; $\mu_n=0.5\text{x}10^{-4}\text{cm}^2\text{V}^{-1}\text{s}^{-1}$,$\mu_p=0.5\text{x}10^{-4}\text{cm}^2\text{V}^{-1}\text{s}^{-1}$.

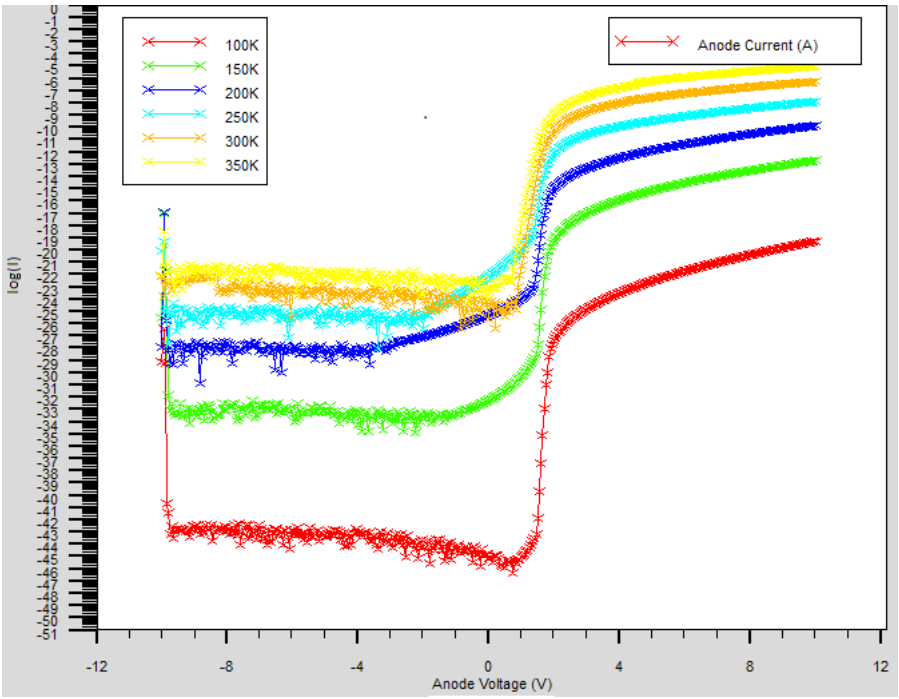

Figure 3.2 : Dark current characteristics for various temperature, Semilog plot.

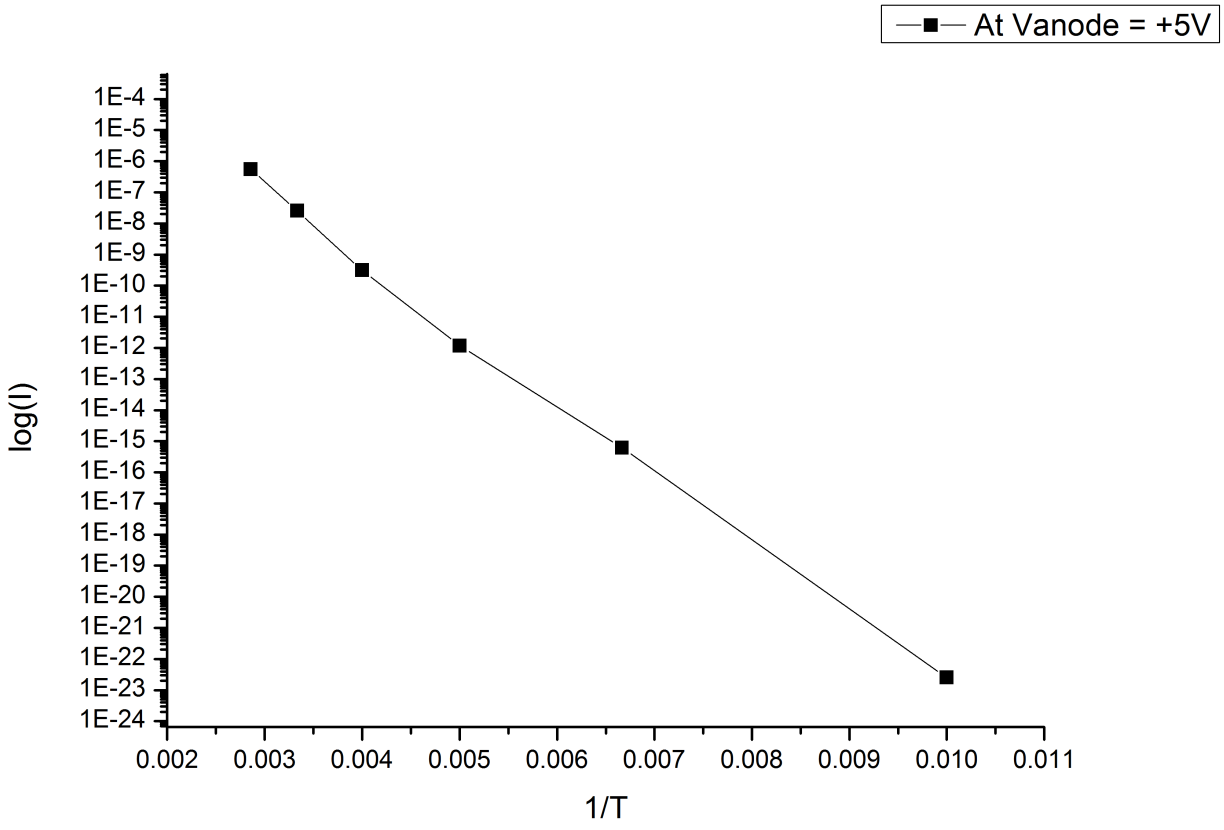

Figure 3.3 : Current vs Temperature for +5V.

Values of current were plotted against temperature, taken at +5V to see its behaviour. It is seen to be approximately a straight line with average slope of -2253.9 , with slope decreasing at lower temperatures. It was not giving a such a linear fit for $(1/T)^2$ case.

3.2 : Contact type and barriers

For this simulation 1μm thick organic layer, having Gaussian Density of states, η_{imag}=1.43 which converts to $\alpha=2x10^{7}m^{-1}$ was used. Work function of anode (W_{fa}) and cathode (W_{fc}) were changed for 3 cases. All parameters for electrons and holes were kept constant otherwise. Light is kept on at $1Wcm^{-2}$. Crandall recombination is switched on. σ_{gauss} = 0.155eV

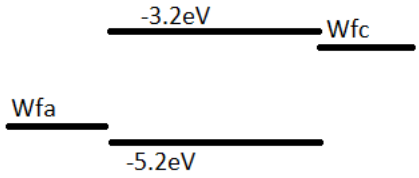

Figure 3.4 : Structure considered for contact effect simulation. Anode-Organic-Cathode

Workfunctions of electrodes, and injection barriers caused thus for forward and reverse bias as mentioned. Ohmic is only for forward bias case, all biases are applied at anode. Cathode is held at 0V. Voltage is sweeped from -5 to +5V

Table 3.1 : Contact workfunctions considered for various cases, and barriers thus formed

Case	W_{fa}	W_{fc}	Barrier Φ_{bf}	Barrier Φ_{bn}
Ohmic	5.2eV	3.2eV	0eV	2eV
Schottky1	4.4eV	4eV	0.8eV	1.2eV
Schottky (mid bg)	4.2eV	4.2eV	1eV	1eV

As can be seen in the following plots, for Ohmic contact the current is 2 orders of magnitude larger than other two cases in forward bias. For Uniform barrier schottky contact, as expected the reverse and forward bias are overlapping. Let $\Phi_d = \Phi_{bn} - \Phi_{bp}$

V_{oc} is seen to be increasing with the separation between workfunction of electrodes, it takes more positive bias to reach flatband condition. Explaining it corresponding to a pn junction, V_{oc} is the voltage applied V_a across the device when the current through the circuit is 0. This happens when the opposite flowing photogenerated current is matched by dark current of pn junction in forward bias ie. $I_{dark} = I_{photogenerated}$. I_{dark} depends upon the voltage drop across the semiconducting layer V_o. And $V_o = V_a - \Phi_d$(in V). So, in case of Ohmic contact where Φ_d is larger more V_a is required for same V_o thus more V_{oc}. But, once it is reached at higher voltages Ohmic contact leads to higher current, then the case where Φ_{bf} =0.8eV then Φ_{bf}=1.0eV. Because the current is injection limited in Schottky cases. As can be thus seen, current for the case of Schottky with Φ_d =0 is 0 at V_{anode} of 0, because the built-in voltage (or V_o) is 0 there.

For negative biases, we are collecting photocurrent and the dark current is less relative to it and is negligible as seen in Figure 3.8. Thus the mentioned injection barriers don't hinder the current. The effect seen in the plot in low negative bias case, that Schottky is seeing less current with respect to Ohmic case is because for each voltage band will be bent more for the case where electrode W_f separation is more, which aids collection by more electric field. But they all are seen to converge at high negative bias, because they see no barrier for collection in any case.

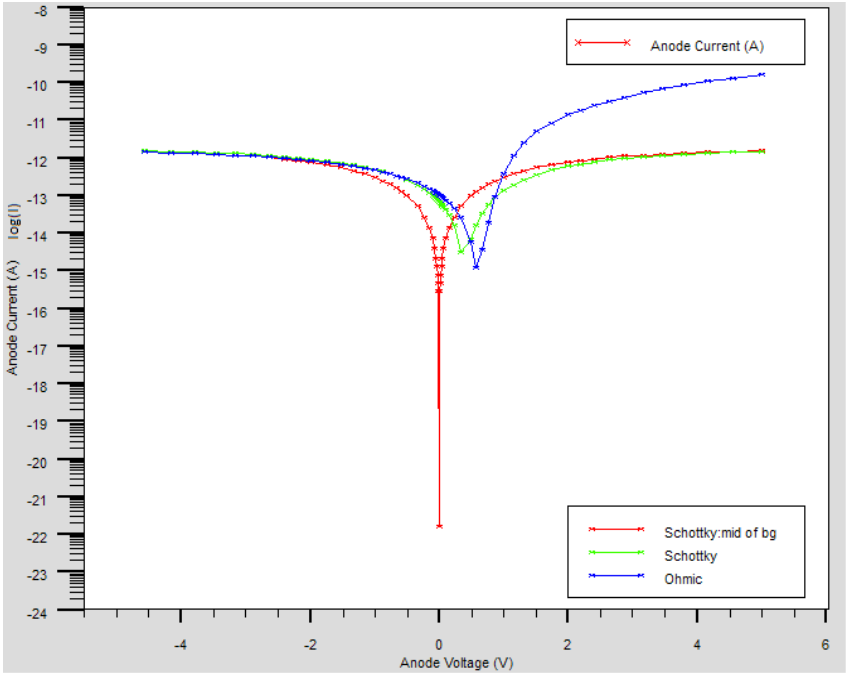

Figure 3.5 : Current Voltage characteristics for each case, plot is on semilog scale

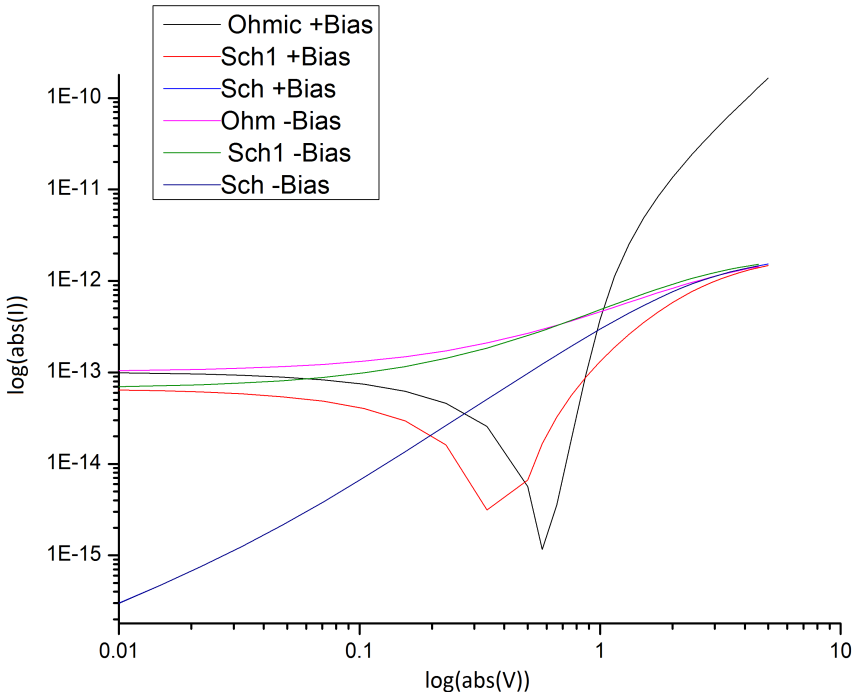

Figure 3.6 : Current voltage characteristics in double logarithmic scale

3.3 : Varying uniform photogeneration and recombination

For this simulations 0.0475µm organic device was used. Gaussian DOS, Pasveer mobility, Crandall recombination used. σ_{gauss} = 0.055eV because we reduced E_g , it was having problems converging at higher σ_{gauss} of 0.155eV

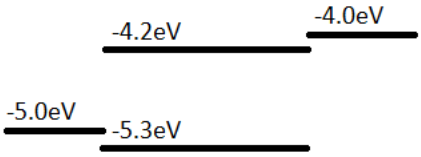

Figure 3.7: Structure considered for constant photogeneration. Anode-Organic-Cathode

As can be seen, anode(left) is kept blocking, while cathode is kept ohmic. For this case, beam was not used but constant photogeneration throughout the device was used, the related file can be found in appendix. Generation rate (G_{ph}) of $1.14x10^{22}$ $cm^{-3}s^{-1}$ was used. Bias at anode is swept from -20V to 20V. This generation rate was multiplied by apropriate factors to obtain the below plots.

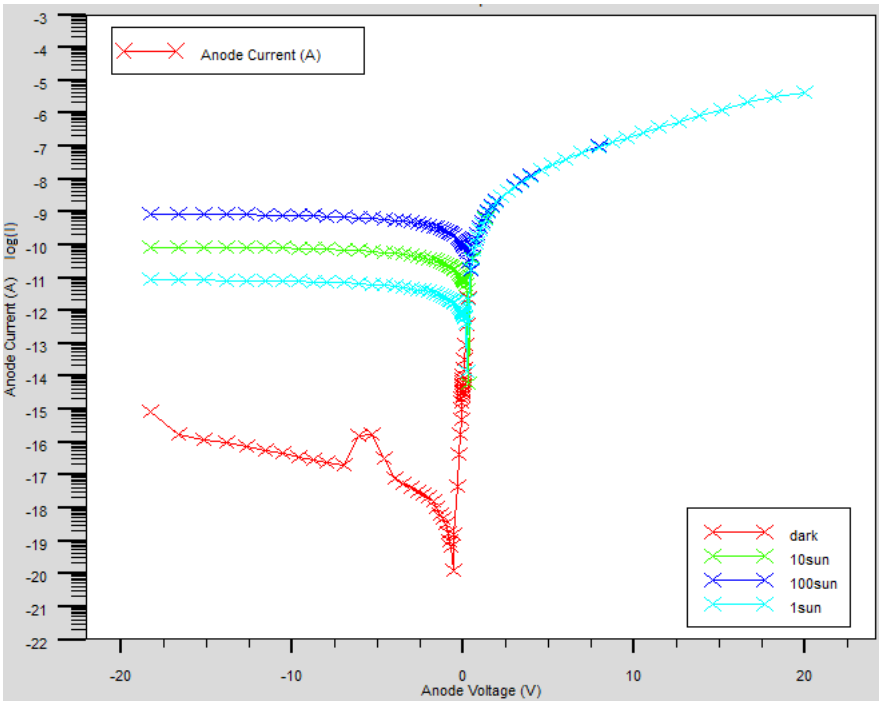

Figure 3.8 : Current voltage characteristics different photogeneration rates. Semilog plot

The plot of recombination within the device is shown below. It is taken at +20v applied at anode(left), and 0V at cathode. Crandall recombination goes to ~0 if either of the carrier's concentration goes to ~0, as can be seen near the contacts. As the cathode is made injecting for

electrons, while anode is slightly blocking for holes; the concentration of electrons at cathode is more than the concentration of holes at anode. Thus, there is a peak in recombination at the cathode end, with respect to anode end. Most of the recombination plots within device at uniform photogeneration behaves like this, as Crandall is the model used throughout the thesis. This is different from the case of minority carrier recombination where $R=\frac{\Delta n}{\tau_n}$ if electrons are the minority carrier, where Δn is excess carrier concentration over equliberium value. Here, the recombination rate depends on both type of carriers and it approaches the form n/τ_n when p>>n

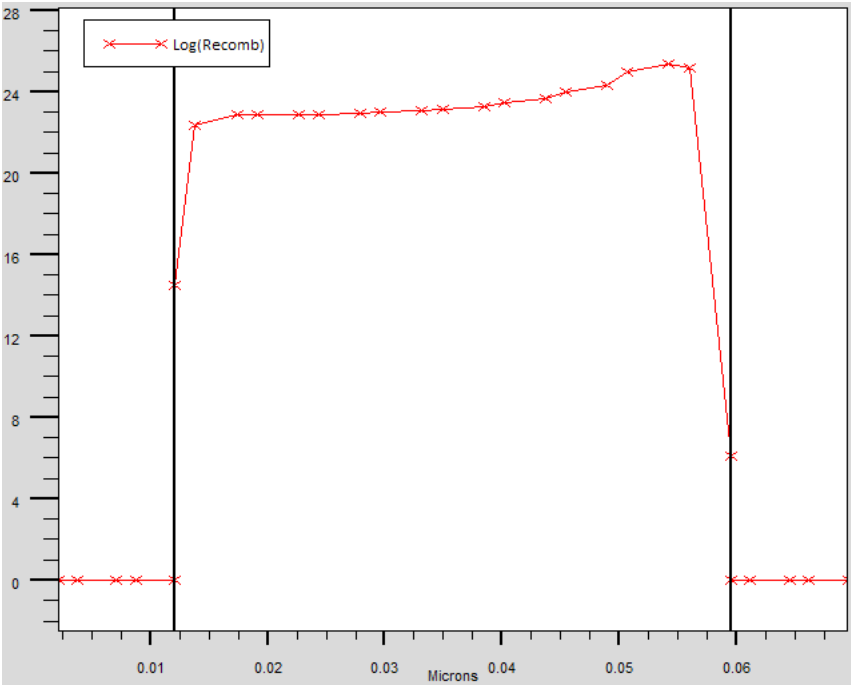

Figure 3.9 : Recombination rate($cm^{-3}s^{-1}$) within the device, Semilog plot.

Table 3.2 : Solar cell specific parameters obtained for constant photogeneration

Intensity	V_{oc}	I_{sc}	Fill Factor
1sun	0.226V	-8.08×10^{-13}A	0.335
10sun	0.338V	-9.13×10^{-12}A	0.306
100sun	0.441V	-9.92×10^{-11}A	0.284

As is seen the open circuit voltage, short circuit current increases as the intensity is increased, while the Fill Factor decreases.

Below is a linear fit of double logarithmic plot of Current versus Intensity for this case. It gives a slope close to 1 for this case of constant photogeneration and crandall recombination, this power law is true for mono-molecular recombination via defects of impurities. The plot was made from the data chosen at two negative voltages.

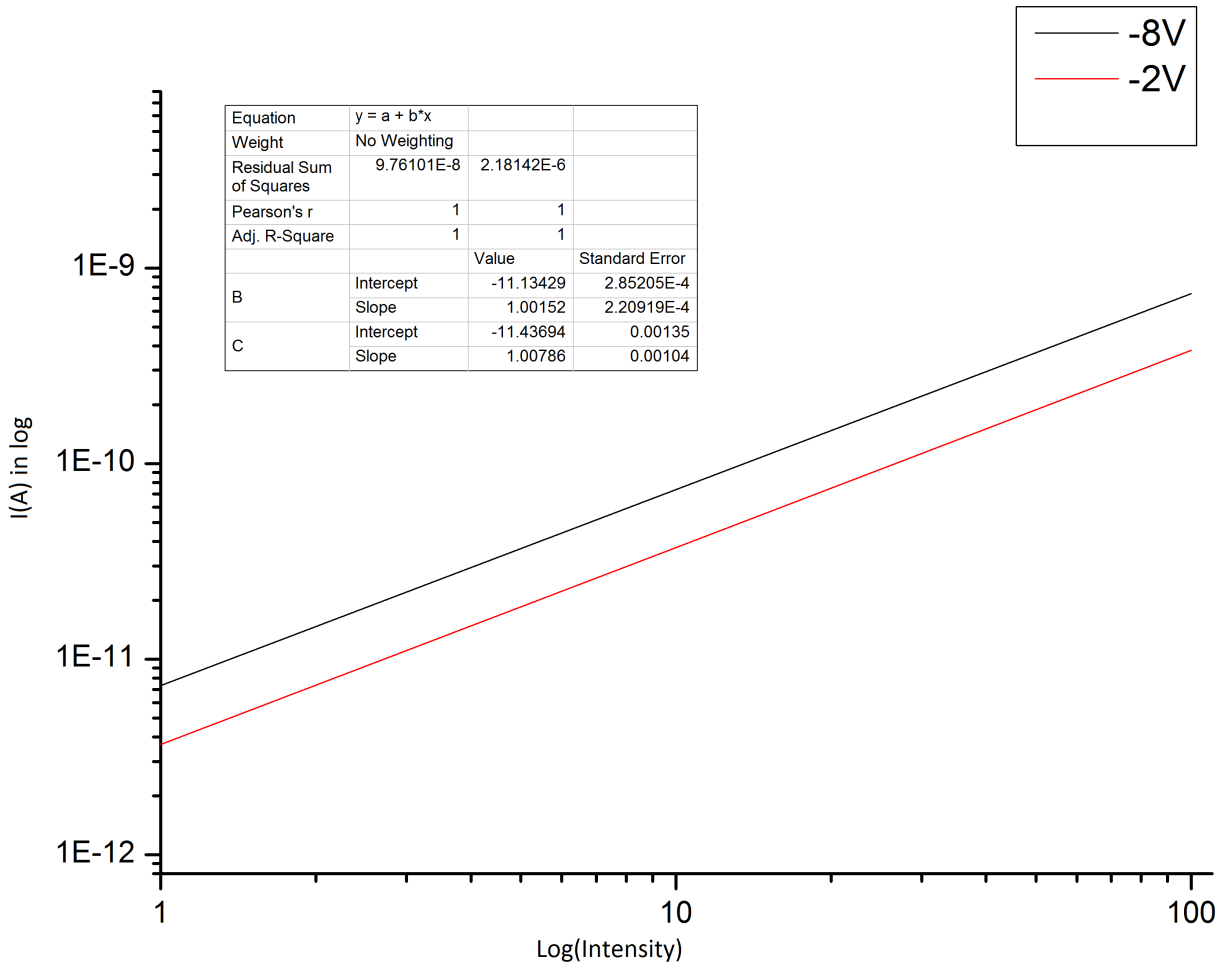

Figure 3.10 : Plot of current vs Intensity, double logarithmic scale

3.4 : Recombination at different voltage bias

For this simulation same material and models as before, namely Crandall, Pasveer are used. The affinity, workfunctions are as shown below. Organic layer's length is 0.0475µm. The anode is on the left, where biases were applied. Also beam was shone from anode towards cathode direction. Values used for the beam were Intensity 1Wcm^{-2}, with α = 2x10^{4}m^{-1} for the material. Meshes were kept nonuniform to detect strange features caused by mesh spacing and contact boundary conditions; thus are caused some of the changes visible in carrier concentration plots. Other differences are caused because one contact is kept ohmic while other blocking. Below are the plots of : 1) Values of various parameters used for the device. 2) Band diagram for +2V and -2V. 3) Electon hole concentration for various biases. 4) Recombination through the device for different bias.*

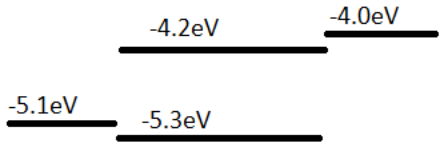

Figure 3.11 : Structure considered for bias' effect on recombination simulation.

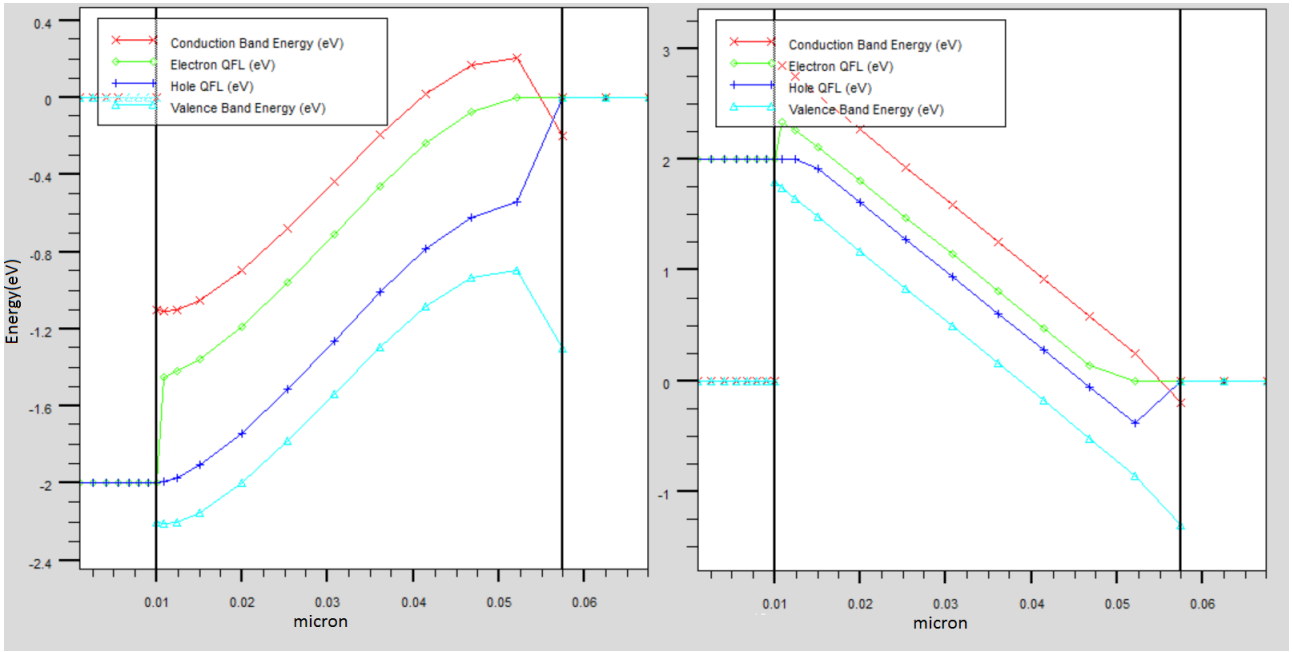

Figure 3.12 : Band diagram for +2V(left) and -2V(right)

*For the recombination plot, slight changes were made. They are 1)Mesh is uniform and density increased. 2) α= 2x10^{5}m^{-1} 3.) Beam intensity = 100Wcm^{-2} 5)Device size rounded off to 0.05µm 6) σ_{gauss} changed to a more appropriate value of 0.08eV

The band diagrams can be explained by theory. For both voltage cases the E_{qfn} crosses the conduction band at the cathode as is expected for the Ohmic contact we have formed. Schottky contact with small barrier is visible at the anode and the difference can be distinctly observed. Also for the forward bias case, the quasifermi levels spread due to more current density which is added upon the photogenerated current density. While it is less for the reverse bias, as the dark current in that case is relatively less. The band bending is as expected. And the carrier concentration plots reflected the band diagram behaviour, as presented below.

We have kept all parameters for electrons and holes equal which is useful to observe any differences caused and figure out the cause. The only non-symmetry of electron and hole plot seen here is due to the ohmic type of contact at cathode for electrons, while schottky contact at anode for holes, this causes the electron concentration at cathode to me more than the hole concentration at the anode. Also as expected the concentration falls off as we go towards other direction, ie. towards anode for electrons. As we go to higher negative bias the concentration is seen as dropping throughout the device except contacts as expected.

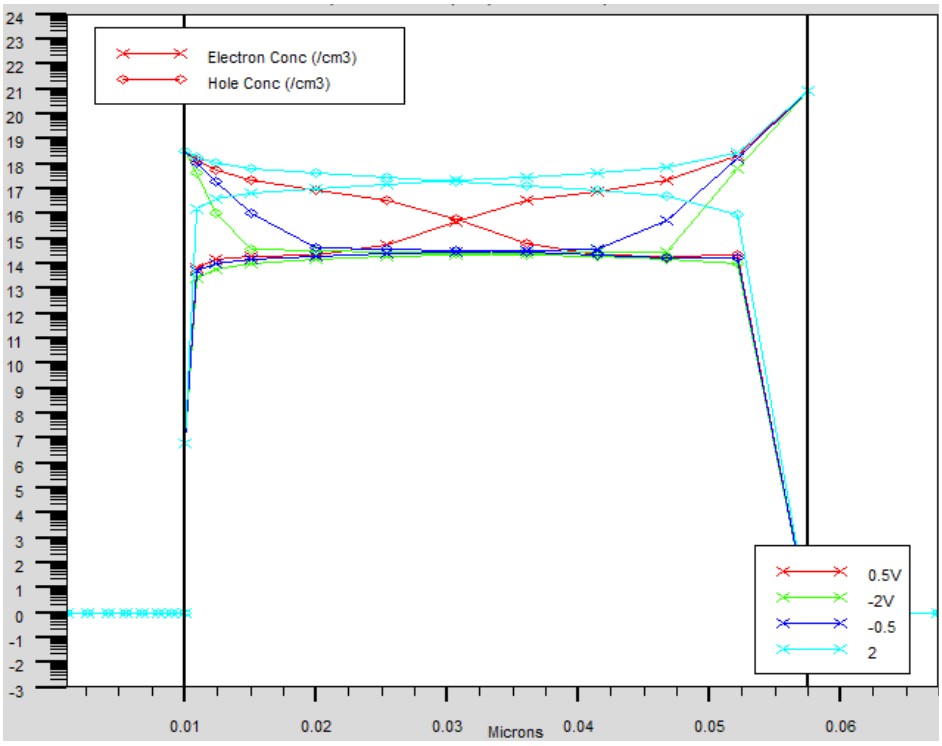

Figure 3.13 : Electron and hole concentration for different biases. Semilog plot

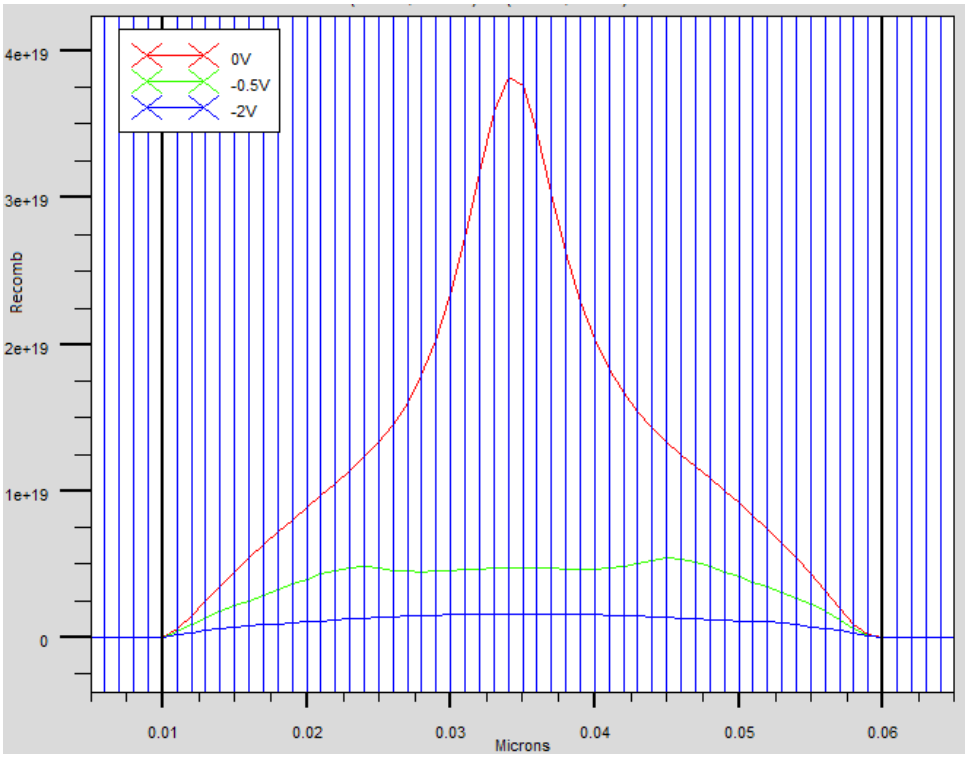

Figure 3.14 : Recombination through the device for different biases; linear plot.

As can be seen in the previous plot, as applied bias increases, recombination decreases. That can be explained as follows. We have set lifetime of the carrier (mentioned in the table) while using Crandall recombination, if we increase the applied bias across the same length of device we are increasing the Electric Field felt by the carrier. This increases carrier's chances to escape the device within it's lifetime and they won't recombine. Hence the observed recombination is less as we go to higher bias.

As modelled in by A. Rose et al. [12] for collecting contacts photocurrent follows power law of $V^{0.5}$ at higher biases before saturating, and V^{1} at lower bias. In his derivation steps concentration of carrier is position dependent and charge neutrality doesnt hold, and he has made similar assumption of recombination happening only in the middle portion for same purposes as mentioned next. The model is considered again in last section.

Also the say the electron generated at the anode end has to travel through the whole device and reach the cathode to be collected. This electron has largest chance to get recombined. Similar for hole produced at the cathode in negative bias. At 0V it is most likely for these carriers (who have spawned in the wrong half of the device) to recombine at the center, and thus we get a peak at the center. At -0.5V their drift velocities are slightly boosted and the peaks are shifted from center to 2 peaks either side and the value is decreased by more than just half. At higher voltages this sharp

peak disappers but still recombination is more at the center than as we go towards the contacts.

This is helped by the spread of concentration of carriers too. Due to the band alignments with respect to contacts, there is low concentration of electrons at anode, and holes at cathode. Hence it is less likely for oppositely charged carrier to recombine as it goes away from the middle of the device. This can be inferred from seeing the carrier plot and examing the n*p values.

3.5 : Effect of device length

For this simulation higher absoption coeffcient $\alpha = 2x10^{6}m^{-1}$ was used to observe difference for considered length scales based on the value of $1/\alpha = 0.5\mu m$, length of the device is varied from $0.5\mu m$ to $2\mu m$. Beam strength is kept constant at $100Wcm^{-2}$.

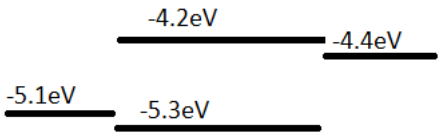

Figure 3.15 : Structure considered for effect of device length simulation.

Photogeneration drops as we go far from anode as the beam is incident there. The difference is an order of magnitude different in $2\mu m$ device at both of it's ends. The drop of photogeneration within the device will be plotted for another similar case later.

For any V_{anode} as the device length increases, the electric field within the device decreases. The electric field stays constant within the device for small lengths, and relatively lower absorption constant.

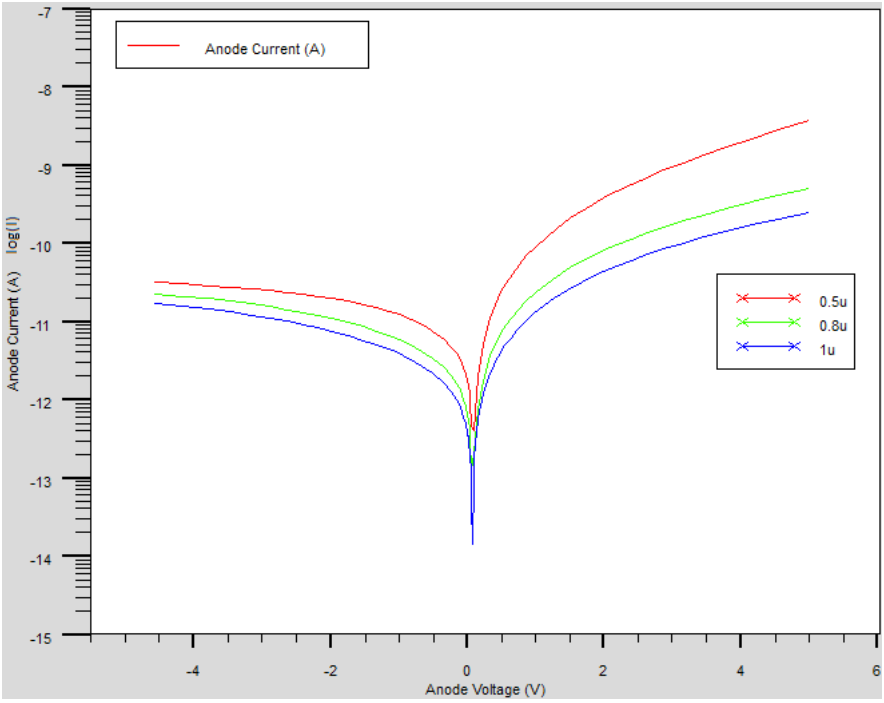

Figure 3.16 : Current voltage characteristics obtained for different device length; semilog scale

Below is the double logarithmic plot of current versus voltage for two device size. Parts of the plot were fit with straight line and slopes were found to determine presence of powerlaw behaviour. The plot shows that it is not a straight line and thus not a simple power law Lower slopes in both cases correspond to negative bias. Note that for both negative bias cases, the mentioned slopes are for the higher section of voltages taken, at lower negative biases slopes are lesser than the mentioned slopes.

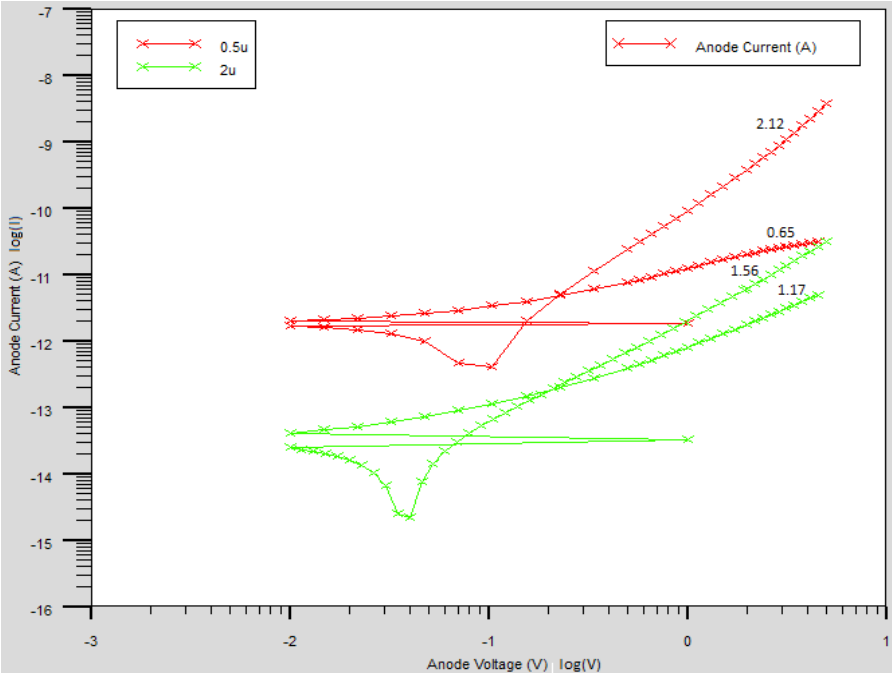

Figure 3.17 : Current voltage characteristics, power law fit for length effect study; log-log scale

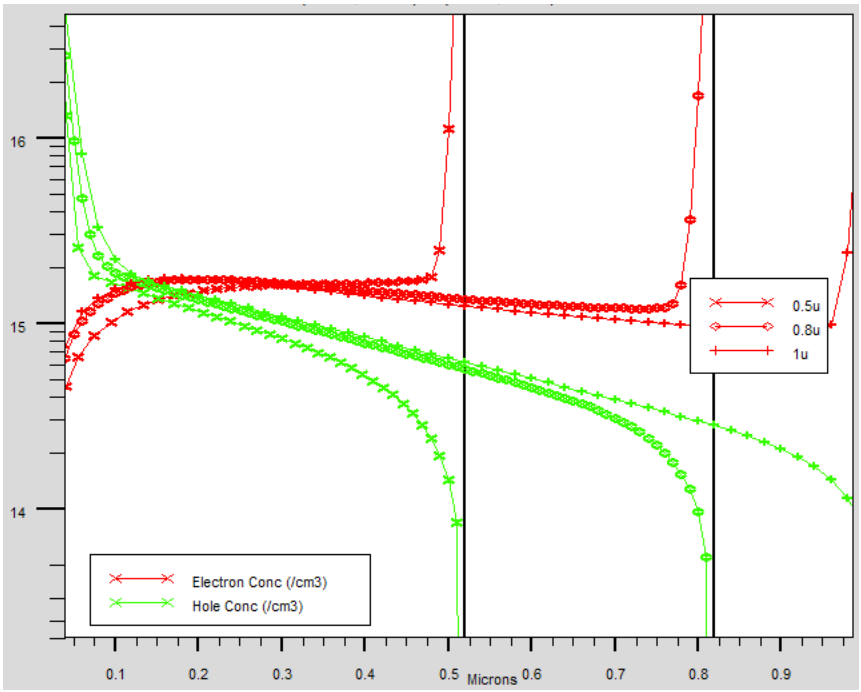

Figure 3.18 : Electron and hole concentration through device(s) overlaid; semilog plot

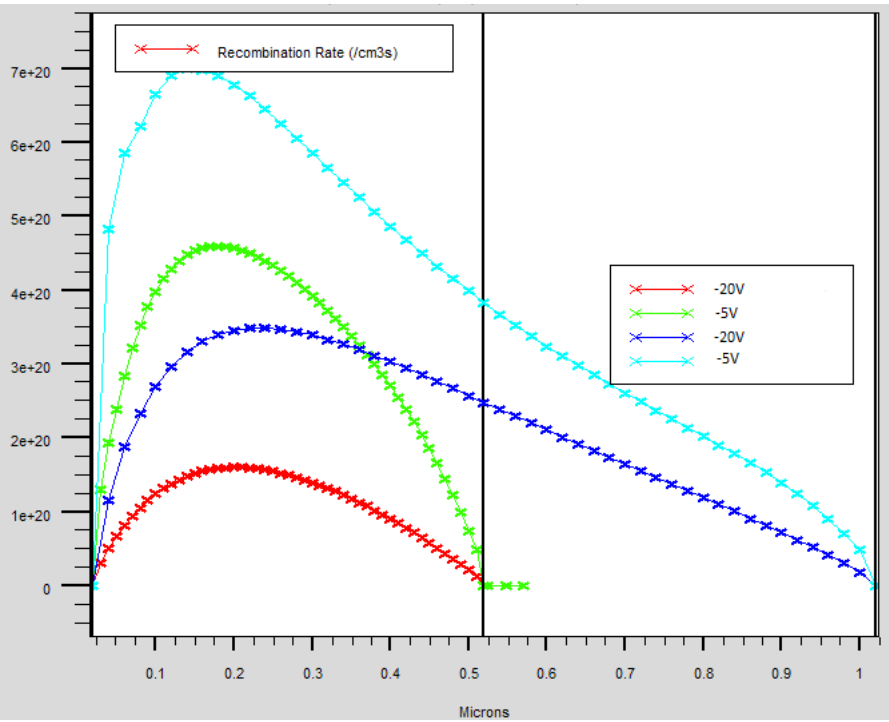

Figure 3.19 : Recombination Rate through the devices at different device length and bias

As can be seen, recombination falls off towards the cathode. This effect will be seen even more enhanced in next section. It's because if you see the carrier concentration plots, it will be observed that hole concentration falls off with x (travelling from anode to cathode), but the electron concentration as much.

Also similar trend as the previous section is followed, recombination decreases as we go deeper into negative bias. J_0 is seen to observe saturation current, it is taken at V_{anode} = -4.16V

Table 3.3 : Solar cell specific parameters obtained for different lengths.

Length(μm)	$J_{AVALIABLE}$(A/μm)	V_{OC}(V)	I_{SC}(A)	Fill Factor	J_0(A)
0.5	5.9×10^{-11}	0.088	-1.45×10^{-12}	0.280	-3×10^{-11}
0.8	7.4×10^{-11}	0.083	-6.94×10^{-13}	0.267	-2.13×10^{-11}
1.0	8.07×10^{-11}	0.077	-4.03×10^{-13}	0.265	-1.5×10^{-11}
2.0	9.17×10^{-11}	0.0376	-3.28×10^{-14}	0.254	-3.75×10^{-12}

The V_{OC}, I_{SC} and Fill Factor decreases as the Length of device is increased.

3.6 : Intensity effect on long device

For this simulation 1μm long layer of organic is considered. To observe enhanced effects high absorption coefficient η_{imag}=1.43 ie. $\alpha=2x10^7 m^{-1}$ is considered. It gives $1/\alpha$ of 50nm. Hence as we move within our device from anode to cathode after a particular x nm photogenerated carriers are less than or comparable to thermally generated carriers, and that portion of device acts as if it is in dark. Same models namely Gaussian Density of states, Pasveer mobility model, and Crandall recombination were considered. Intensity of beam incident at anode was varied from 0.01Wcm^{-2} to 1000Wcm in steps of increasing order. And at each Intensity voltage sweep was done, and IV characteristics obtained. Also carrier concentration, recombination, energy bands were studied at many conditions. Some of the results will be presented below.

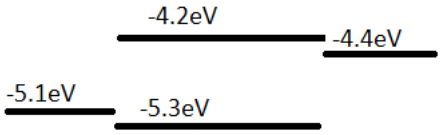

Figure 3.20 : Device considered for Intensity effect

We will take values of current at -4.56V for all six intensities, and plot log(current) vs log(Intensity) the plot shows the fit and slopes obtained. As can be seen, for intensities from 0.01Wcm^{-2} to 10Wcm^{-2} the slope if current vs intensity is approximately 1, and for the intensities 10Wcm^{-2} to 1000Wcm^{-2} the slope is 0.33.

As is noted in the below plot, for higher intensities the reverse bias current doesnt saturate as it normally does otherwise.

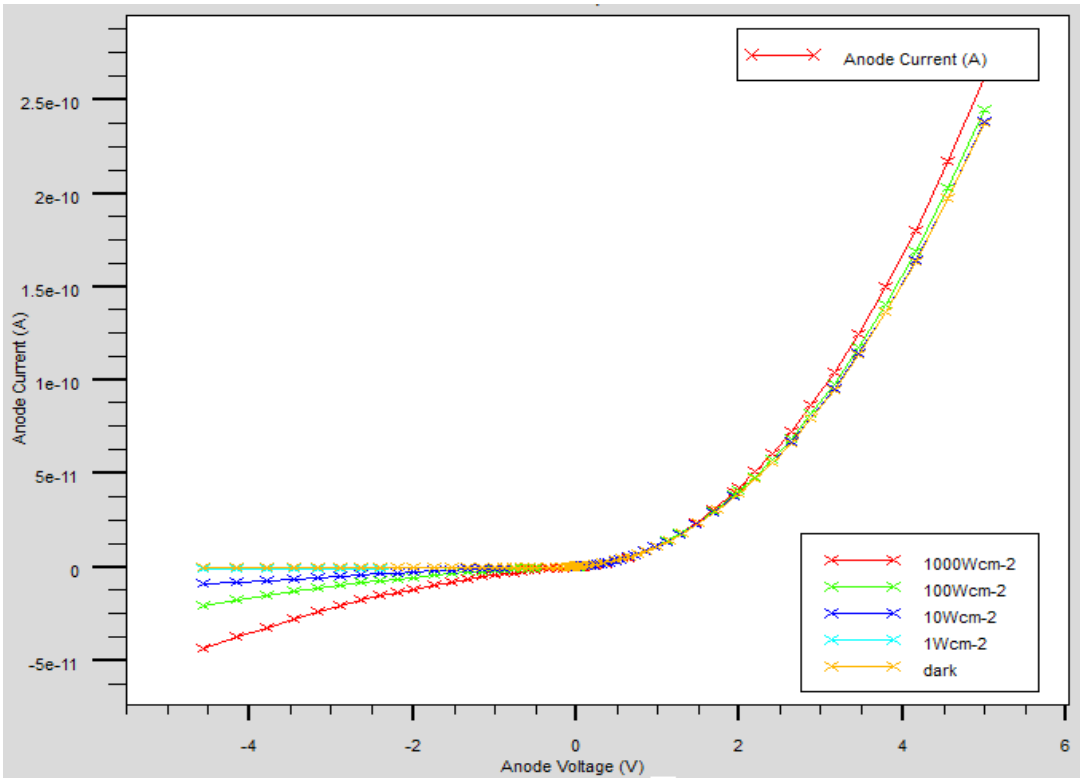

Figure 3.21 : Current voltage (linear scale) observed for different intensities

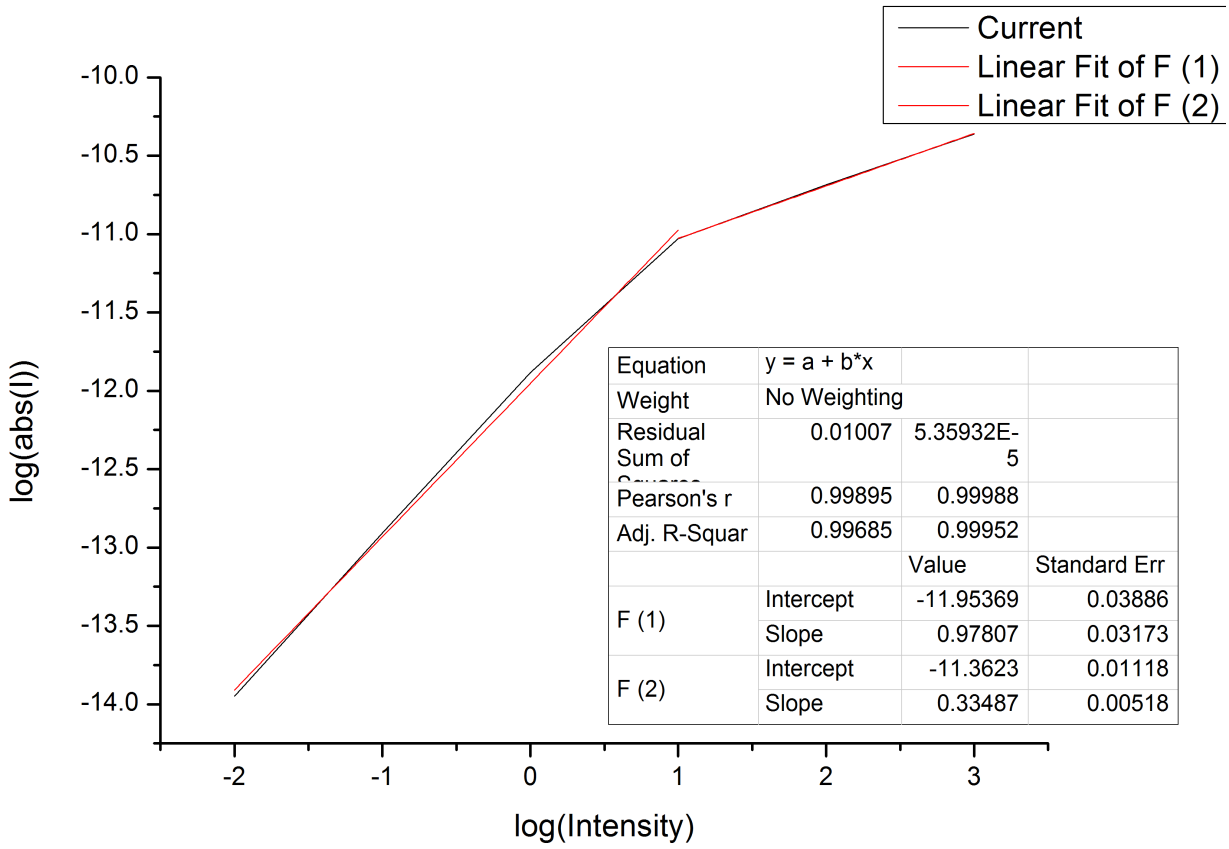

Figure 3.22 : Current versus Intensity (double logathmic) plot and linear fit for different Intensity range

As mentioned by L.J.A. Koster et al.[13] Non-linear Intensity dependence of short circuit current is speculated to arise from the losses in the form of bimolecular recombination (which has $I = kV^{0.5}$) behaviour or due to the build up of space charge due to the difference in mobilities. For our case we have not taken into account bimolecular recombination.

Below are the band diagram and carrier concentration plots they are taken when 0V is applied at anode, but note that the workfunctions of metals are different. General trends are followed that is carrier concentration is more for high intensity. If the bands are observed at -20V the $1Wcm^{-2}$ doesnt do what it does here and follows the trend of other intensities.

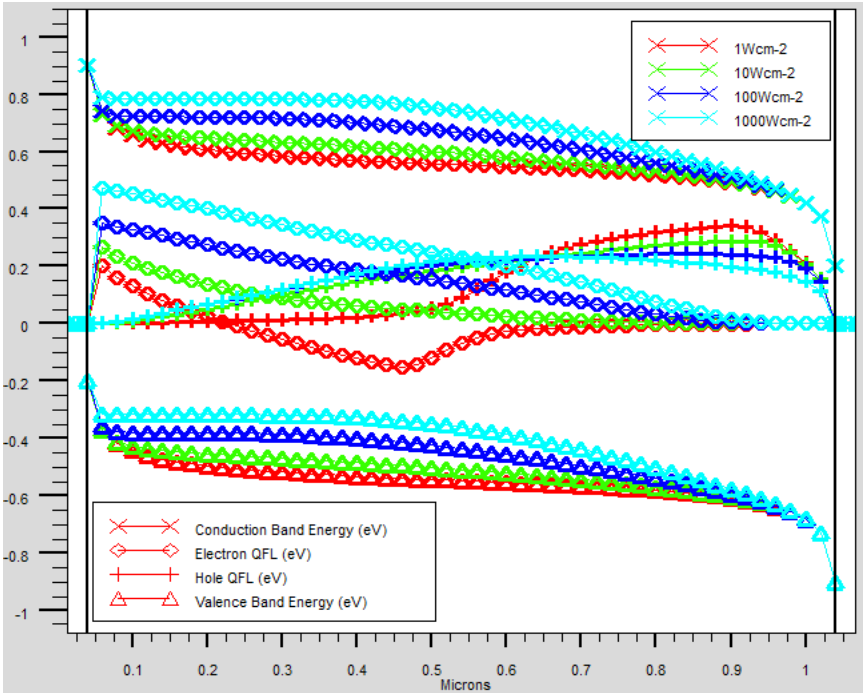

Figure 3.23 : Band diagram within the device for different intensities; taken at 0V

As modelled in the paper by Rose et al.[12] say if there are more trapped electrons than holes in any particular region, ie. the case of net charge trapping, electric field starts to distort until there is no net charge trapping, and thus equal current density of holes and electrons is collected out of both contacts. Similar effect can be seen here. As seen in the next plot, there is excess of electrons within the device. At cathode electrons are collected for negative bias. This makes the bands bend more in cathode region to extract electrons more effectively. And also the slope of band at the anode is less, to maintain holes within device. This changes the electric field within the device as seen in the following plots. It is more in the cathode end than at the anode end. This is happening because of high intensities, and long device such that half of the device is in darkness, it is giving rise to space charge limited current in the left half of the device where photogeneration is very high. As derived for space charge the power law $I = kG^{0.75}$ where G is Generation rate or Intensity.Figure 3.24 :

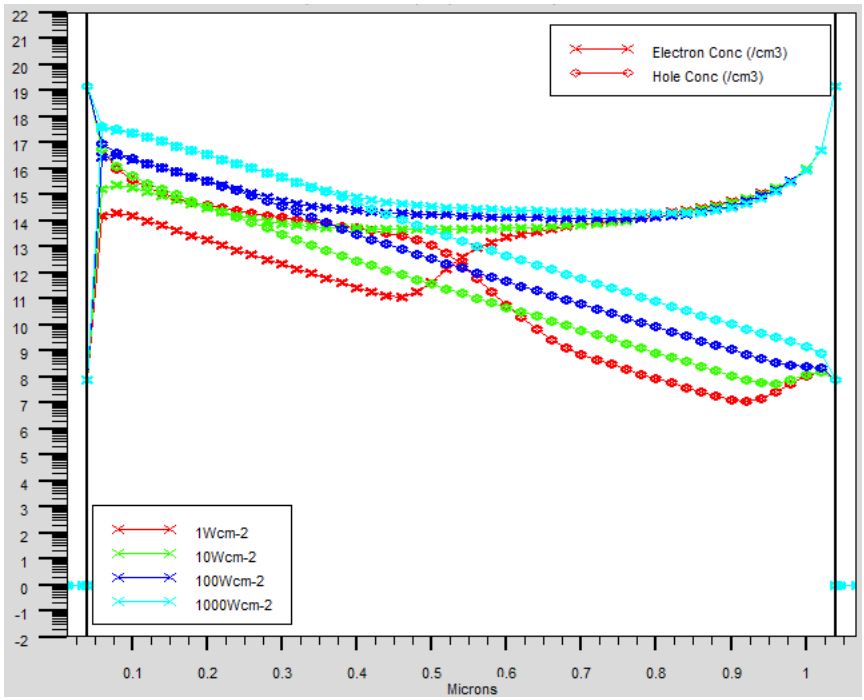

Electron and hole concentration within device for varying intensity; taken at 0V

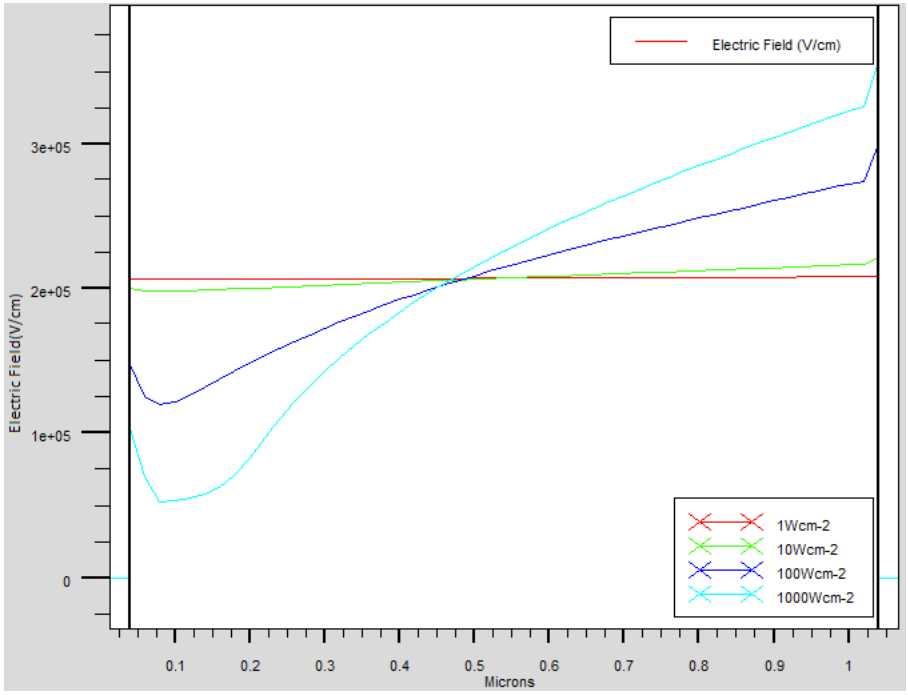

Figure 3.25 : Electric field within the device for varying intensity; taken at -20V

As noted the field is distorted for higher intensities such that it is less at the anode side, and more at the cathode side to enhance electron collection relative to hole collection out of electrodes. Also, the field is less distorted as we go to lower intensities, and is absent at 0.01Wcm^{-2}. This may be because of having to compensate for higher photogeneration at higher intensities and thus higher charged carriers causing the effect decribed in relation to Rose et al. The field distortion observed for higher voltages was more than for lower voltages.

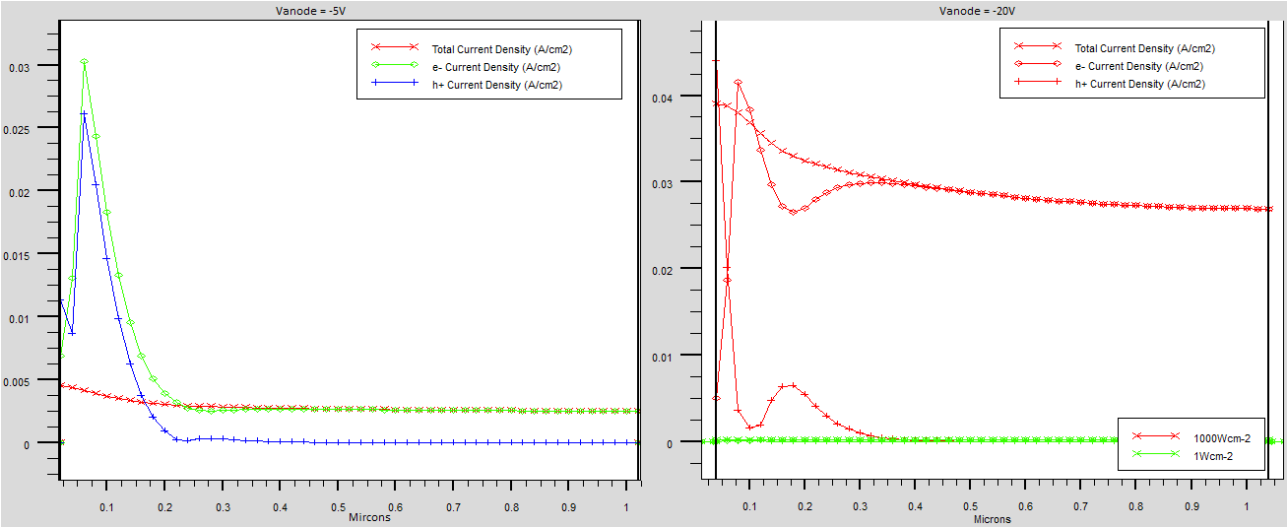

Figure 3.26 : Current density within the device; taken at -5V(left) and -20V(right)

This final plot shows that the current density is not uniform within the device. The left and right plots are for 1000Wcm^{-2} . As noted earlier distortion of electric field is caused as a counter to net charge trapping and non equal current density anode and cathode. For these two cases, we calculate the amount of distortion to current density as $\delta_J = \frac{J_{max} - J_{min}}{J_{min}}$, note that J_{min} is the part which stays relatively uniform in the right part of device. We find that $\delta_{J,-5V} = 0.8$ while $\delta_{J,-20V} = 0.44$. This current density behaviour suggests charging in the device at higher intensities(at lower intensities 0.01Wcm^{-2} it was negligible, and for shorter devices with uniform photogeneration in earlier simulations, it was absent.).

Although note that derivation as mentioned in Rose et al[12] doesn't take into account Poisson equation, and the field behaviour is determined solely based on Current continuity across two layers in which Field is different, and based on carrier recombination length ($\mu_n\tau_n$). The device is divided into 3 regions, as follows : 1) Electrons are extracted at the positive contact, and no recombination in this region because drift length of electrons is more than the length of this region $l_1 = \mu_n \tau_n E_1$; 2) Generation = Recombination is assumed in this region $l_2 = l - l_1 - l_3$; 3) Holes are extracted at the negative contact, no recombination is again assumed, and length decided based on it $l_3 = \mu_p \tau_p E$. After this J_p and J_n are calculated in each region, and made continuous across the boundaries of these regions. For the relation exact equation derived the reader is direced to the reference, but the current voltage is seen to follow different power law in different regime in case of non-equal mobilites; linear regime at low volage I = kV, intermediate voltages, high voltage and squareroot power law $I = k'V^{0.5}$, very high voltage and saturation regime I = constant. Finally space charge effect has also been discussed obtaining an analytical form of

$J = egl_1, \quad where\, l_1 = (V^{1/2}/g^{1/4})$. Thus the Intensity power law of $I=kg^{0.75}$, and voltage dependence of $I=k'V^{0.5}$ was predicted for spacecharge limited case.

As can be seen in the Figure 3.17, where we tried to calculate slope of log(I) vs log(V) for short as well as long device, we found out that it doesnt follow a fixed power law – that the slope is not constant over voltages- as suggested by work of Rose et al.. And that the current voltage dependence is not simply of powerlaw nature. A better model is thus required. Slopes greater than one can be explained by mobility having a Electric Field term (as in Poole Frenkel effect).

Also can be seen in this section, inspite of having same lifetime*mobility term for both carriers, in which case as per the work of Rose et. al. we should only see Linear and saturation regime, we see presence of space charge; although we must note that parts of our device are in dark, and only parts illuminated, as we have taken a high absorption coefficient case. While in their work they hadn't considered non-uniform photogeneration and it's effect on the operation of device.

CHAPTER 4
CONCLUSION

We started with a non-Gaussian DOS, and obtained a behaviour where current was decreasing with temperature. Next we introduced Gaussian DOS, and hopping mobility and recombination models, studying Ohmic versus Schottky barriers, finding the current decreasing with the increasing injection barrier across the metal semiconductor contact. Also, was seen it's diminished effect in reverse bias. We now studied the recombination rate through the device under constant photogeneration, and the increase in the reverse bias current with photogeneration increase. Also simulation results were fitted to obtain linear variation of current versus intensity as expected for the models we have considered. Next we obtained decrease in the rate of recombination with increase in negative bias as expect. We further went to change the device size, observing the behaviour of recombination, and it's effect on Fill Factor. Finally we considered a long device, nonuniform photogeneration, and observed intensity effecs on current over a large range. At lower intensity it behaved as expected in a linear manner, but at higher intensities distortion of electric field as proposed by others, space charge effect was seen. Throughout the thesis we had maintained same property values for electrons and holes, and that helped us observe the effect of changing each parameter clearly.

APPENDIX A
ATLAS CODE

1 : SOURCE CODE TO SIMULATE DEVICE

```
##############################################################
# Run for IV characteristics
go atlas
# title Device Characteristics of Organic solar cell

# Change the material thickness here
set Organic_Thick=1.0
set Anode_Thick=0.05
set Cathode_Thick=0.05

set Total_Thick=$Organic_Thick + $Cathode_Thick

# Number of steps taken while sweeping bias
set nstep=10

# Mesh definition
mesh   smooth=1 space.mult=1.0
x.mesh l= 0.0  spacing=1
x.mesh l=10.0  spacing=1

y.mesh l=-$Anode_Thick    spacing=0.02
y.mesh l=-0.005          spacing=0.02
y.mesh l=0.0            spacing=0.02
y.mesh l=$Organic_Thick     spacing=0.02
y.mesh l=$Organic_Thick+0.005       spacing=0.02
y.mesh l=$Total_Thick spacing=0.02

# Region and electrodes specification
region num=1    material=organic    y.min=0.0 y.max=$Organic_Thick
```

```
elec   num=1   name=anode  x.min=0 x.max=10.0 y.min=-$Anode_Thick \
                  y.max=0
elec   num=2   name=cathode x.min=0 x.max=10.0 y.min=$Organic_Thick \
                   y.max=$Total_Thick



# Set parameters for Organic Layer. f.recomb specifies recombination model used.
material region=1 material=organic \
       eg300=1.1 ntc.gauss=8.51e20 sigc.gauss=0.08 ntv.gauss=8.51e20 \
                 sigv.gauss=0.08 permittivity=3.0 affinity=4.2 imag.index=1.43 \
                 f.recomb=recomb.lib

# This piece of code is used if we want to use parabolic DOS
#material region=1 material=organic \
#       eg300=1.1 permittivity=3.0 nc300=2.5e19 nv300=2.5e19 affinity=4.2 \
#                         imag.index=1.43E-01 f.recomb=recomb.lib


# Defining mobility parameters for Organic layer

# This piece of code is used if we want to use constant mobility.
#mobility mup=1.0e-4 mun=1.0e-4

# This piece of code is used if we want to use Poole Frenkel mobility model.
#mobility region=1 material=organic  deltaen.pfmob=0.48 deltaep.pfmob=0.48 \
#         betan.pfmob=3.7e-4 betap.pfmob=3.7e-4 mun=0.5e-5 mup=0.5e-4

# Setting parameters for Pasveer model of mobility.
mobility mup=1.0e-4 mun=1.0e-4 pasveer.n ccutoff.n=1 fcutoff.n=10 \
         pasveer.p ccutoff.p=1 fcutoff.p=10
```

```
# This can be used to simulate constant photo-generation. f.radiate describes
# photo-generation in terms of spatial coordinates
#beam num=1 f.radiate=solarex07.lib

# This simulates a beam of light incident at the anode.
BEAM NUM=1 WAVELENGTH=0.9 X.ORIGIN=5.0 Y.ORIGIN=-0.06 ANG=90.0
MIN.WINDOW=-0.1 MAX.WINDOW=0.1
#output opt.int

# Calcium (Cathode)
contact name=cathode workfunc=4.4
# ITO (Anode)
contact name=anode workfunc=5.1

#Analytic parameter is used to switch on Caughey Thomas model
#model langevin analytic print
model print

#This can be used to alter numerical solving parameters.
#method climit=1e-4 maxtrap=0

# Saving the structure of device
save outfile=cell.str

# Specifies various probes within the device

#probe field max x=5 name="Electric Field"
output recomb con.band val.band e.mob h.mob
probe y=0.02 x=5.0 n.conc name="n.conc"
probe y=0.02 x=5.0 dir=90 n.mob name="n.mob"
probe y=$Organic_Thick-0.01 x=5.0 name="inten" beam=1 intensity

solve init
solve prev
```

```
#b1 is in W/cm^2
#
# Switch on the sun
#
solve b1=0.01

# Bias sweep
solve vanode=-20
save outfile=organiceV_20.str
solve vanode=-15
save outfile=organicV_15.str
solve vanode=-10
save outfile=organicV_10.str
solve vanode=-5
save outfile=organicV_5.str

log outfile=organicex05_0_light.log
set v7=-5
set v8=-2
set s6=exp(log($v8/$v7) / $nstep)
solve vstep=$s6 vmult vfinal=$v8 name=anode
save outfile=organicex05_V_2.str
set v9=-0.5
set s7=exp(log($v9/$v8) / $nstep)
solve vstep=$s7 vmult vfinal=$v9 name=anode
save outfile=organicex05_V_05.str
set v10=-0.01
set s8=exp(log($v10/$v9) / $nstep)
solve vstep=$s8 vmult vfinal=$v10 name=anode

solve vanode=0
save outfile=organicex05_V0.str
extract name="V1" max(abs(v."anode"))
```

```
set v1=0.01
set v2=0.5
set s1=exp(log($v2/$v1) / $nstep)
solve vanode=0.01 vstep=$s1 vmult vfinal=$v2 name=anode
save outfile=organicex05_V05.str
set v3=2
set s2=exp(log($v3/$v2) / $nstep)
solve vstep=$s2 vmult vfinal=$v3 name=anode
save outfile=organicex05_V2.str
set v4=5
set s3=exp(log($v4/$v3) / $nstep)
solve vstep=$s3 vmult vfinal=$v4 name=anode
save outfile=organicex01_V5.str

# Extracting various parameters.
extract name="short_circuit_current" y.val from curve(v."anode", i."anode") where x.val=0
extract name="open_circuit_voltage" x.val from curve(v."anode", i."anode") where y.val=0
extract name="Power" curve(v."anode", (v."anode" * i."anode" *(-1))) \
      outf="P.dat"
extract name="Pmax" max(curve(v."anode", (v."anode" * i."anode" *(-1))))
extract name="V_Pmax" x.val from curve(v."anode", (v."anode"*i."anode"))\
         where y.val=(-1)*$"Pmax"
extract name="Fill Factor" ($"Pmax"/($"short_circuit_current"*$"open_circuit_voltage"))
extract name="intens" max(probe."inten")
extract name="Eff" ($Pmax/($"intens"*20/1e8))

# Plotting current voltage characteristics
tonyplot organicex05_0_light.log
tonyplot P.dat

quit
```

2 : RECOMBINATION MODEL FILE

```
#include <stdio.h>
#include <stdlib.h>
#include <math.h>
#include <ctype.h>
#include <malloc.h>
#include <string.h>
#include <template.h>

int recomb(double xcomp,double ycomp,double temp,double n,double p,double *r,double
*drdn,double *drdp,double *drdl)
{
        *r = ((n*p)/((n*(1e-06))+(p*(1e-06))));
        *drdn = ((p*p*(1e-06))/((n+p)*(n+p)*(1e-06)*(1e-06)));
        *drdp = ((n*n*(1e-06))/((n+p)*(n+p)*(1e-06)*(1e-06)));
        return(0);              /* 0 - ok */
}
```

3 : CONSTANT PHOTOGENERATION FILE

```
#include <stdio.h>
#include <stdlib.h>
#include <math.h>
#include <ctype.h>
#include <malloc.h>
#include <string.h>
#include <template.h>

int radiate(double x, double y, double z, double t, double *rat)
{
        *rat = 2.7e21;
        return(0);              /* 0 - ok */
}
```

REFERENCES

1. Nir Tessler, Yevgeni Preezant et al. Charge Transport in Disordered Organic Materials and Its Relevance to Thin-Film Devices: A Tutorial Review, Adv. Mater. 2009, 21, 2741–27611

2. M. Ali Omar (1993) Elementary Solid State Physics : Principles and Applications, Addison-Wesley Publishing Company

3. Zhenan Bao, Jason Locklin (2007) Organic Field-Effect Transistors, Taylor and Franicis Group

4. D. M. Caughey, R. E. Thomas, Carrier Mobilities in Silicon Empirically Related to Doping and Field, Proceedings of the IEEE,Dec. 1967

5. H. Bassler , Charge Transport in Disordered Organic Photoconductors A Monte Carlo Simulation Study, Phys. stat. sol. (b) 175, 15(1993)

6. W. F. Pasveer, J. Cottaar, et. al , Unified Description of Charge-Carrier Mobilities in Disordered Semiconducting Polymers, PhysRevLett 94,206601(2005)

7. Atlas User's Manual Device Simulation Software (2013), Silvaco, Inc.

9. R. S. Crandall, Modeling of thin film solar cells: Uniform field approximation, Journal of Applied Physics 54, 7176 (1983);

10. Dr. Roderick MacKenzie, Recombination in organic solar cells, 8/2011

11. Mott, Nevill F.; Gurney, R. W. (1940). Electronic Processes in Ionic Crystals, 1st ed. Oxford University Press.

12. Alvin M. Goodman and Albert Rose, Double Extraction of Uniformly Generated Electron Hole Pairs from Insulators with Noninjecting Contacts, Journal of Applied Physics, 1971

13. L. J. A. Koster, V. D. Mihailetchi, H. Xie, and P. W. M. Blom, Origin of the light intensity dependence of the short-circuit current of polymer/fullerene solar cells, Applied Physics Letters 87, 203502 (2005)

14. Simon M. Sze, Physics of Semiconductor Devices, 3rd Edition, Wiley, 2006

15. Ben G. Streetman, Sanjay Banerjee, Solid State Electronic Devices, Pearson Prentice Hall, 2006

16. Ben Minnaert and Marc Burgelman, Modelling MEH-PPV:PCBM (1:4) bulk heterojunction solar cells, Numos 2007, pp. 327–339